RHEOLOGY AND RHEOLOGICAL MEASUREMENTS

1. Introduction

Rheology is the science of the deformation and flow of matter. It is concerned with the response of materials to applied stress. That response may be irreversible viscous flow, reversible elastic deformation, or a combination of the two. Control of rheology is essential for the manufacture and handling of numerous materials and products, eg, foods, cosmetics, rubber, plastics, paints, inks, and drilling muds. Before control can be achieved, there must be an understanding of rheology and an ability to measure rheological properties.

Deformation is the relative displacement of points of a body. It can be divided into two types: flow and elasticity. Flow is irreversible deformation; when the stress is removed, the material does not revert to its original form. This means that work is converted to heat. Elasticity is reversible deformation; the deformed body recovers its original shape, and the applied work is largely recoverable. Viscoelastic materials show both flow and elasticity.

This article is concerned with rheological measurements on both liquids and solids and the principles on which they are based. The flow properties of a liquid are defined by its resistance to flow, ie, viscosity, and may be measured by determining the rate of flow through a capillary, the resistance to flow when the fluid is sheared between two surfaces, or the rate of motion of an object or ball moving through the fluid. The mechanical properties of an elastic solid may be studied by applying a stress and measuring the deformation or strain. Many solids, such as polymers, undergo flow in addition to recoverable elastic deformation. Furthermore, a number of liquids show elastic as well as flow behavior. These materials are viscoelastic, and additional techniques beyond those indicated for solids and liquids are needed for complete characterization. Examples of such methods are the measurement of response to sinusoidal oscillatory motion; the measurement of flow with time after application of stress, ie, creep; and the measurement of the rate and degree of recovery after removal of stress, ie, creep recovery or recoil.

In addition to viscometers, optical devices such as microscopes and cameras can be used for defining and solving flow problems as well as characterizing materials (1–3). Optical techniques allow the investigator to determine the physical structure of the material and visualize its flow processes.

2. Viscosity

A liquid is a material that continues to deform as long as it is subjected to a tensile and/or shear stress. The latter is a force applied tangentially to the material. In a liquid, shear stress produces a sliding of one infinitesimal layer over another, resulting in a stack-of-cards type of flow (Fig. 1).

For a liquid under shear, the rate of deformation or shear rate is a function of the shearing stress. The original exposition of this relationship is Newton's

law, which states that the ratio of the stress to the shear rate is a constant, ie, the viscosity. Under Newton's law, viscosity is independent of shear rate. This is true for ideal or Newtonian liquids, but the viscosities of many liquids, particularly a number of those of interest to industry, are not independent of shear rate. These non-Newtonian liquids may be classified according to their viscosity behavior as a function of shear rate. Many exhibit shear thinning, whereas others give shear thickening. Some liquids at rest appear to behave like solids until the shear stress exceeds a certain value, called the yield stress, after which they flow readily.

Some commonly observed types of flow behavior are shown in Figure 2, in which the shear stress is plotted against shear rate. These plots are called flow curves and are frequently used to express the rheological behavior of liquids. Newtonian flow is shown by a straight line, and shear thinning and thickening by curves. Yield stresses, τ_0, are shown by intercepts on the stress (y) axis. It should be pointed out that the existence of yield stresses is controversial; they may be artifacts resulting from high Newtonian viscosity at low shear rates (4). However, in many dispersed systems, particularly where severe flocculation occurs, this viscosity is so high that the material would take years to flow. Therefore, in practice, there are true yield stresses. This parameter can be quite useful in characterizing materials. Additional information on yield is available (5–8).

Viscosity is equal to the slope of the flow curve, $\eta = d\tau/d\dot{\gamma}$. The quantity $\tau/\dot{\gamma}$ is the viscosity η for a Newtonian liquid and the apparent viscosity η_a for a non-Newtonian liquid. The kinematic viscosity is the viscosity coefficient divided by the density, $\nu = \eta/\rho$. The fluidity is the reciprocal of the viscosity, $\phi = 1/\eta$. The common units for viscosity, dyne seconds per square centimeter ((dyn·s)/cm^2) or grams per centimeter second ((g/(cm·s)), called poise, which is usually expressed as centipoise (cP), have been replaced by the SI units of pascal seconds, ie, Pa·s and mPa·s, where 1 mPa = 1 cP. In the same manner the shear stress units of dynes per square centimeter, dyn/cm^2, have been replaced by Pascals, where 10 dyn/cm^2 = 1 Pa, and newtons per square meter, where 1 N/m^2 = 1 Pa. Shear rate is $\Delta V/\Delta X$, or length/time/length, so that values are given as per second (s^{-1}) in both systems. The SI units for kinematic viscosity are square centimeters per second (cm^2/s), ie, Stokes (St), and square millimeters per second (mm^2/s), ie, centistokes (cSt). Information is available for the official Society of Rheology nomenclature and units for a wide range of rheological parameters (9).

2.1. Flow Models. Many flow models have been proposed (8–10), which are useful for the treatment of experimental data or for describing flow behavior (Table 1). However, it is likely that no given model fits the rheological behavior of a material over an extended shear rate range. Nevertheless, these models are useful for summarizing rheological data and are frequently encountered in the literature.

Of the models listed in Table 1, the Newtonian is the simplest. It fits water, solvents, and many polymer solutions over a wide strain rate range. The plastic or Bingham body model predicts constant plastic viscosity above a yield stress. This model works for a number of dispersions, including some pigment pastes. Yield stress, τ_0, and plastic (Bingham) viscosity, $\eta_p = (\tau - \tau_0)\gamma$, may be determined from the intercept and the slope beyond the intercept, respectively, of a shear stress vs shear rate plot.

The other models can be applied to non-Newtonian materials where time-dependent effects are absent. This situation encompasses many technically important materials from polymer solutions to lattices, pigment slurries, and polymer melts. At high shear rates most of these materials tend to a Newtonian viscosity limit. At low shear rates they tend either to a yield point or to a low shear Newtonian limiting viscosity. At intermediate shear rates, the power law or the Casson model is a useful approximation.

The power law, $\tau = k\dot{\gamma}^n$, is widely used as a model for non-Newtonian fluids. It holds for many solutions and can describe Newtonian, shear-thinning, and shear-thickening behavior, depending on the power factor, n, also called the flow behavior index. For a Newtonian fluid, $n = 1$ and the equation reduces to the Newtonian model. If n is less than 1, the fluid is shear thinning; if it is greater than 1, the fluid is shear thickening. A test of whether the power law applies and a means of determining n is to plot the log shear stress vs the log shear rate. If the plot is linear, the power law applies. The value of n, which is the reciprocal of the slope of the line, can be used as a measure of the degree of shear thinning or shear thickening. Dividing the power law equation through by $\dot{\gamma}$ gives an expression in terms of viscosity, $\eta = k'\dot{\gamma}^{n-1}$.

The power law model can be extended by including the yield value $\tau - \tau_0 = k\dot{\gamma}^n$, which is called the Herschel–Bulkley model, or by adding the Newtonian limiting viscosity η_∞. The latter is done in the Sisko model, $\eta_\infty + k\dot{\gamma}^{n-1}$. These two models, along with the Newtonian, Bingham, and Casson models, are often included in data-fitting software supplied for the newer computer-driven viscometers.

Another model is the Casson equation (11), which is useful in establishing the flow characteristics of inks, paints, and other dispersions. An early form of this expression (eq. 1) was modified (12) to give equation 2.

$$\tau^{1/2} = k_0 + k_1\dot{\gamma}^{1/2} \tag{1}$$

$$\eta^{1/2} = \eta_\infty^{1/2} + \tau_0^{1/2}\dot{\gamma}^{-1/2} \tag{2}$$

The square root of viscosity is plotted against the reciprocal of the square root of shear rate (Fig. 3). The square of the slope is τ_0, the yield stress; the square of the intercept is η_∞, the viscosity at infinite shear rate. No material actually experiences an infinite shear rate, but η_∞ is a good representation of the condition where all rheological structure has been broken down. The Casson yield stress τ_0 is somewhat different from the yield stress discussed earlier in that there may or may not be an intercept on the shear stress–shear rate curve for the material. If there is an intercept, then the Casson yield stress is quite close to that value. If there is no intercept, but the material is shear thinning, a Casson plot gives a value for τ_0 that is indicative of the degree of shear thinning.

The Williamson equation is useful for modeling shear-thinning fluids over a wide range of shear rates (13). It makes provision for limiting low and high shear Newtonian viscosity behavior (eq. 3), where τ is the absolute value of the shear stress and τ_m is the shear stress at which the viscosity is the mean of the viscosity limits η_0 and η_∞, ie, at $\eta = (\eta_0 + \eta)_\infty/2$.

$$\eta = \eta_\infty + \frac{\eta_0 - \eta_\infty}{1 + (|\tau|\tau_m)} \tag{3}$$

The Cross equation assumes that a shear-thinning fluid has high and low shear-limiting viscosity (14) (eq. 4), where α and n are constants.

$$\eta = \eta_\infty + \frac{\eta_0 - \eta_\infty}{1 + \alpha\gamma^n} \tag{4}$$

The value for n is often given as 2/3, but polymer melts have shown a wide range of values. The constant α is associated with rupture of the linkages in the structure of the fluid. The effect of different values of α, ie, at the same values of η_0 and η_∞, is shown in Figure 4. As α increases, breakdown occurs at lower and lower shear rates.

2.2. Thixotropy and Other Time Effects. In addition to the nonideal behavior described, many fluids exhibit time-dependent effects. Some fluids increase in viscosity (*rheopexy*) or decrease in viscosity (*thixotropy*) with time when sheared at a constant shear rate. These effects can occur in fluids with or without yield values. Rheopexy is a rare phenomenon, but thixotropic fluids are common. Examples of thixotropic materials are starch pastes, gelatin, mayonnaise, drilling muds, and latex paints. The thixotropic effect is shown in Figure 5, where the curves are for a specimen exposed first to increasing and then to decreasing shear rates. Because of the decrease in viscosity with time as well as shear rate, the up-and-down flow curves do not superimpose. Instead, they form a hysteresis loop, often called a thixotropic loop. Because flow curves for thixotropic or rheopectic liquids depend on the shear history of the sample, different curves for the same material can be obtained, depending on the experimental procedure.

Experimentally, it is sometimes difficult to detect differences between a shear-thinning liquid in which the viscosity decreases with increasing shear, and a thixotropic material in which the viscosity decreases with time, because of the combined shear and time effects that occur during a series of measurements. This is especially true if only a few data points are collected. In addition, most materials that are thixotropic are also shear thinning. In fact, one definition of a thixotropic fluid limits it to materials whose viscosity is a function of both shear rate and time (8).

Viscosity–time measurements during or after shearing can be used to show time-dependent effects. The plots in Figure 6 (15) are representative of the results of such measurements on a thixotropic material. On shearing at a given shear rate, the viscosity drops sharply at first, but the rate of change continually decreases until a constant or nearly constant level is reached. This is sometimes referred to as the sheared state. Changing to a higher shear rate causes a a further drop in viscosity. When the shear rate is reduced, the viscosity increases quickly at first, and then increases more slowly. A good example of this is the behavior of latex house paint. The shearing plot represents the brushing action, whereas the recovery plot shows what happens when the brushing stops. The thixotropic behavior allows the paint to be easily brushed to a thin film and

gives a short period of time for the brush marks to level; then the viscosity increase prevents running and sagging.

Causes of time-dependent behavior include irreversible changes such as cross-linking, coagulation, degradation, and mechanical instability, and reversible changes involving the breaking and re-forming of colloidal aggregations and networks. Models of time-dependent behavior are less satisfactory and more controversial than those of shear-dependent behavior. Few comprehensive investigations of the viscosity–shear–time profiles of thixotropic and rheopectic materials have been published, but there are sources that contain good discussions of thixotropy (15–17). Rheopexy has also been described (18,19).

Time-dependent effects are measured by determining the decay of shear stress as a function of time at one or more constant shear rates (20). Sequential increases in shear rate followed by equilibration allows the shear stress to reach a maximum value and then decrease exponentially toward an equilibrium level. The peak shear stress, which is obtained by extrapolating the curve to zero time, and the equilibrium shear stress are indicative of the viscosity–shear behavior of unsheared and sheared material, respectively. The stress–decay curves are indicative of the time-dependent behavior. A rate constant for the relaxation process can be determined at each shear rate. In addition, zero-time and equilibrium shear stress values can be used to construct a hysteresis loop that is similar to that shown in Figure 5, but unlike that plot, is independent of acceleration and time of shear.

Another method is the step-shear test (15), which uses controlled shearing and the recovery behavior shown in Figure 6 to characterize the material. In this method, a high shear rate ($\sim 10^4\ s^{-1}$) is applied to the specimen until the viscosity falls to an equilibrium value. The shear rate then is reduced to a low value ($\sim 1\ s^{-1}$), allowing the structure to re-form and the viscosity to recover. The data can be analyzed in a number of ways. The time it takes to achieve 50% viscosity recovery or some other fraction of the original value can be used to indicate the rate of recovery. Comparisons can be made based on these times or on the time needed to reach a given viscosity. Equation 5 has been fit to the recovery curve, where $\eta\ (t)$ is the viscosity as a function of time, t; $\eta_{t=0}$, the sheared-out viscosity at recovery time zero; $\eta_{t=\infty}$, the infinite time recovered viscosity; and τ, a time constant describing the recovery rate.

$$\eta(t) = \eta_{t=0} + (\eta_{t=\infty} - \eta_{t=0})(1 - e^{-t/\tau}) \tag{5}$$

Another method for estimating thixotropy involves the hysteresis of the thixotropic loop. The area of the thixotropic loop is calculated or measured, which works well with printing inks (1). In a variation of this method, the up curve on an undisturbed sample is determined. The sample is then sheared at high shear ($>2000\ s^{-1}$) for 30–60 s, followed by determination of the down curve (21). The data are plotted as Casson–Asbeck plots, $\eta^{1/2}$ vs $\dot{\gamma}^{-1/2}$ (12). Such plots are best used for comparison and ranking, but a measure of the degree of thixotropy can be gained by determining the angle formed by the two lines or the area of the triangle formed by the lines and a vertical line through a given value for

$\gamma \cdot^{-1/2}$. Additional methods for determining the degree of thixotropy have been described (7).

Results from measurements of time-dependent effects depend on the sample history and experimental conditions and should be considered approximate. For example, the state of an unsheared or undisturbed sample is a function of its previous shear history and the length of time since it underwent shear. The area of a thixotropic loop depends on the shear range covered, the rate of shear acceleration, and the length of time at the highest shear rate. However, measurements of time-dependent behavior can be useful in evaluating and comparing a number of industrial products and in solving flow problems.

2.3. Effect of Temperature. In addition to being often dependent on parameters such as shear stress, shear rate, and time, viscosity is highly sensitive to changes in temperature. Most materials decrease in viscosity as temperature increases. The dependence is logarithmic and can be substantial, up to 10% change/°C. This has important implications for processing and handling of materials and for viscosity measurement.

A common expression relating viscosity to temperature is the Arrhenius equation, $\eta = A \times e^{B/T}$ or $\eta = A \times 10^{B/T}$, where A and B are constants characteristic of the polymer or other material, and T is the absolute temperature. Estimation of the viscosity of a polymer at a given temperature requires a knowledge of the viscosity at two other temperatures. This knowledge allows calculation of the constants A and B and subsequent determination of viscosities at other, intermediate temperatures.

The Arrhenius equation may also be expressed in logarithmic form (eq. 6):

$$\log \eta = \log A + B/T \tag{6}$$

For two temperatures (viscosity known at one), this expression may be written as follows (eq. 7):

$$\log(\eta_1/\eta_2) = B\left(\frac{1}{T_1} - \frac{1}{T_2}\right) \tag{7}$$

In practice, plots of $\log \eta$ vs $1/T$ tend to be straight lines over a considerable range of values. Such plots may be used to predict viscosity at one temperature from viscosities at other temperatures. Likewise, previously measured viscosity–temperature curves for commerical products are often used to ensure meaningful viscosity data for quality assurance even where temperature control is not possilbe.

The Arrhenius equation holds for many solutions and for polymer melts well above their glass-transition temperatures. For polymers closer to their T_g and for concentrated polymer and oligomer solutions, the Williams–Landel–Ferry (WLF) equation (22) works better (23,24). With a proper choice of reference temperature T_s, the ratio of the viscosity to the viscosity at the reference temperature can be expressed as a single universal equation (eq. 8):

$$\log(\eta/\eta_s) = \frac{-8.86(T - T_s)}{101.6 + (T - T_g)} \tag{8}$$

Because T_s is often defined as $T_g + 50$ K, the equation thus becomes

$$\log(\eta/\eta_g) = \frac{-17.4(T - T_g)}{51.6 + (T - T_g)}$$

In general, the WLF equation holds over the temperature range T_g to $(T_g + 100^\circ C)$.

2.4. Dilute Polymer Solutions. The measurement of dilute solution viscosities of polymers is widely used for polymer characterization. Very low concentrations reduce intermolecular interactions and allow measurement of polymer–solvent interactions. These measurements are usually made in capillary viscometers, some of which have provisions for direct dilution of the polymer solution. The key viscosity parameter for polymer characterization is the limiting viscosity number or intrinsic viscosity, $[\eta]$. It is calculated by extrapolation of the viscosity number (reduced viscosity) or the logarithmic viscosity number (inherent viscosity) to zero concentration.

The *viscosity ratio* or *relative viscosity*, η_{rel}, is the ratio of the viscosity of the polymer solution to the viscosity of the pure solvent. In capillary viscometer measurements, the relative viscosity (dimensionless) is the ratio of the flow time for the solution t to the flow time for the solvent t_0 (Table 2). The specific (sp) viscosity (dimensionless) is also defined in Table 2, as is the viscosity number or reduced (red) viscosity, which has the units of cubic meters per kilogram (m^3/kg) or deciliters per gram (dL/g). The logarithmic viscosity number or inherent (inh) viscosity likewise has the units m^3/kg or dL/g. For η_{red} and η_{inh}, c, the concentration of polymer, is expressed in convenient units, traditionally g/100 cm^3 but kg/m^3 in SI units. The viscosity number and logarithmic viscosity number vary with concentration, but each can be extrapolated to zero concentration to give the limiting viscosity number (intrinsic viscosity) (Table 2). Usually, measurements at four or five concentrations are needed.

The specific viscosity can also be represented by (25)

$$\eta_{sp} = [\eta]c + k_1[\eta]^2c^3$$

which becomes the Huggins equation (26)

$$\eta_{sp}/c = [\eta](1 - k_h[\eta]c)$$

where k_h is the Huggins viscosity constant, the most commonly used dilute solution viscosity number or index. It is easily determined from the slope of a plot of η_{sp}/c vs c such as the lower plot in Figure 8. The Huggins constant can be thought of as a measure of the "goodness" of the solvent for the polymer with values around 0.3 in good solvents and 0.5–1 in theta solvents. A large number of Huggins constants can be found in Reference (25) along with constants for another

semiempirical equation relating viscosity and concentration, that of Schulz and Blaschke (27).

The Huggins equation and Huggins constants can be used to determine values for $[\eta]$ (28,29). The latter gives an equation

$$[\eta] = (1 + 4k_n\eta_{sp})^{1/2} - 1/2k_nc$$

that can be used for single-point determinations (calculations from a single viscosity measurement at a known concentration). The general validity of single-point methods has been questioned, however (30). An even simpler but equally useful method is to approximate $[\eta]$ by the logarithmic viscosity number of a single sufficiently dilute solution: $[\eta]\eta_{inh} = (\ln \eta_{rel})/c$, where $c = 1–2$ kg/m^3 or 0.1–0.2 g/100 cm^3.

The limiting viscosity number depends on the polymer, solvent, and temperature, but under a given set of conditions it is related to the molecular weight by the Mark–Houwink relation, $[\eta] = KM^a$, where K and a are constants and M is the molecular weight of the polymer. Tables of K and a are available for a large number of polymers and solvents (31,32). Excellent summaries of equations, techniques, and references relating to the viscosity of dilute polymer solutions are also available (33,34), as is information on dilute polymer solutions that are shear thinning (35).

2.5. Concentrated Polymer Solutions. Knowledge of the viscosity behavior of concentrated solutions (36–38) is important to the manufacture and application of caulks, adhesives, inks, paints, and varnishes. It is also useful for designing and controlling polymer manufacturing processes, fiber spinning, and film casting. Viscosity behavior can be investigated by a variety of methods, including the use of simple capillary viscometers, extrusion rheometers, and rotational viscometers. Unlike dilute solutions, concentrated polymer solutions show a vast amount of interaction between the macromolecules. The degree of interaction is governed by the concentration, the characteristics of the chains, and the nature of the solvent. A convenient measure of concentration is the dimensionless reduced concentration $\tilde{c}$, which is the product of the concentration and the limiting viscosity number (intrinsic viscosity) $[\eta]$ (36). The transition from dilute to concentrated solutions occurs at a critical concentration c_c and corresponds to c values of several units. In addition, at a critical molecular weight, where $M > M_c$ and $c > c_c$, a fluctuating entanglement network forms. For a concentrated solution, properties above and below M_c may be quite different. For example, the dependence of viscosity on molecular weight, which is much greater in concentrated than in dilute solutions, changes from a value on the order of unity below M_c to one of 3.4–3.5 above M_c (37,39,40). That is, $\eta = KM$ below M_c and $\eta = KM^{3.4–3.5}$ above M_c. Viscosity in these expressions should be the zero-shear viscosity η_0, but because the relationships hold for low shear measurements in many cases, the notation remains in the more general form η.

The break point above which entanglement occurs varies widely with molecular structure; a range of 3,800–36,000 molecular weight has been shown (41). In highly concentrated oligomeric solutions such as high solids organic coatings (volume fraction > 0.7), high dependencies of viscosity on molecular weight occur

even at low molecular weights (42–44). This is probably on account of hydrogen bonding that causes the stringing together of short chains or the formation of a loose network, thereby increasing the effective chain length. Something similar to this has been seen with the formation of viscosity-building needle-like structures by low molecular weight materials (45).

Depending on the concentration, the solvent, and the shear rate of measurement, concentrated polymer solutions may give wide ranges of viscosity and appear to be Newtonian or non-Newtonian. The shear rate at which the break in behavior occurs depends on the concentration and on the solvent.

2.6. Melt Viscosity. The study of the viscosity of polymer melts (46–57) is important for the manufacturer who must supply suitable materials and for the fabrication engineer who must select polymers and fabrication methods. Thus, melt viscosity as a function of temperature, pressure, rate of flow, and polymer molecular weight and structure is of considerable practical importance. Polymer melts exhibit elastic as well as viscous properties. This is evident in the swell of the polymer melt upon emergence from an extrusion die, a behavior that results from the recovery of stored elastic energy plus normal stress effects. Theoretical developments include a constitutive equation that correctly captures nonlinear behavior in both elongation and shear (58,59).

A number of experimental methods have been applied to measure the melt viscosity of polymers (51–60), but capillary extrusion techniques probably are generally preferred. Rotational methods are also used, and some permit the measurement of normal stress effects resulting from elasticity as well as of viscosity. Slit rheometers can also be used to measure normal stress (61). Oscillatory shear measurements are useful for measuring the elasticity of polymer melts (52,53). Controlled stress methods have also been applied (54). Squeeze film flow has also been proposed as a geometry suitable for processibility testing of polymer melts (55). Nonlinear viscoelastic behavior is found in many molten plastics. Theoretical (62) as well as practical approaches address this issue, including a sliding plate normal-thrust rheometer (63,64).

Polymer melts show a low shear rate Newtonian limit and a region of diminishing viscosity with increasing shear rate. Although it is likely that a high shear rate Newtonian region exists, this has generally not been observed experimentally because of the effects of heat generation and polymer degradation at high shear rates.

The limiting low shear or zero-shear viscosity η_0 of the molten polymer can be related to its weight-average molecular weight M_w by the same relations noted for concentrated solutions: $\eta_0 = KM_w$ for low molecular weight and $\eta_0 = KM_w^{3.5}$ for high molecular weight.

The transition between two forms of behavior occurs at a critical molecular weight M_c, which corresponds to a critical chain length, Z_c. The transition is clearly shown in Figure 7, which is a plot of Newtonian viscosity vs chain length in terms of carbon atoms for a series of molten polyethylenes (34). This transition is thought to be related to chain fluctuations in the polymer melt in such a way that the motion changes from displacement of whole chains to restricted motion called *reptation*, ie, wiggly, snake-like motion within the tight tube formed by the matrix of neighboring chains (65–67). Polymer entanglement and reptation have

considerable influences on melt rheology, particularly on viscoelasticity, with many consequences for the molding and extrusion of plastics.

The viscosity–molecular weight relationships noted above hold for narrow molecular weight distribution polymers. For polymers having broad molecular weight distributions, viscosity depends on a molecular weight average between M_w and the next higher average M_z (z average), approaching M_z as the distribution broadens. Branching can have a considerable effect, reducing or increasing the viscosity depending on the ratio of the length of the branch to the entanglement length (68). The flow curve for a polymer melt can be predicted from the molecular weight distribution (69) and, under some circumstances, a molecular weight distribution can be determined from the flow curve (70,71). As might be expected, fillers also have an effect on melt viscosity (72).

The dependence of viscosity on temperature is critical to the handling of molten polymers in molding, extrusion, and other manufacturing processes. In fact, the drop in viscosity with increasing temperature makes these operations possible. Therefore, viscosity–temperature relationships are important. Data for many polymers can be found in the literature (46–51). The behavior of others can be determined by viscosity measurements over a range of temperatures. Viscosity–stress master curves are useful in the prediction of viscosity at a given temperature (73). The viscosity–stress curves shown in Figure 8 (46) are approximately superimposable by shifting at constant stress.

The temperature dependence of melt viscosity at temperatures considerably above T_g approximates an exponential function of the Arrhenius type. However, near the glass transition the viscosity temperature relationship for many polymers is in better agreement with the WLF treatment (22).

Melt viscosity is also affected by pressure (46,74,75). The compression of a melt reduces the free volume and therefore raises the viscosity. For example, the viscosity of low density polyethylene increases by a factor of roughly 10 over a static pressure range of 34–170 MPa (5,000–25,000 psi).

2.7. Dispersed Systems. Many fluids of commercial and biological importance are dispersed systems, such as solids suspended in liquids (dispersions) and liquid–liquid suspensions (emulsions). Examples of the former include inks, paints, pigment slurries, and concrete; examples of the latter include mayonnaise, butter, margarine, oil-and-vinegar salad dressing, and milk. Dispersion of a solid or liquid in a liquid affects the viscosity. In many cases Newtonian flow behavior is transformed into non-Newtonian flow behavior. Shear thinning results from the ability of the solid particles or liquid droplets to come together to form network structures when at rest or under low shear. With increasing shear the interlinked structure gradually breaks down, and the resistance to flow decreases. The viscosity of a dispersed system depends on hydrodynamic interactions between particles or droplets and the liquid, particle–particle interactions (bumping), and interparticle attractions that promote the formation of aggregates, flocs, and networks.

Emulsions have not been studied as thoroughly as dispersions, probably because of the greater complexity of the former. Emulsions tend to be unstable, and frequently droplets begin to coalesce soon after the emulsion forms. Thus the emulsion is continually changing. In addition, droplets may change shape under

shear or when packed tightly together. This makes it difficult to apply theories developed for solid spheres or other well-defined geometries of shape.

Detailed treatments of the rheology of various dispersed systems are available (76–81), as are reviews of the viscous, elastic, and yield behavior of dispersions (82–85), of the flow properties of concentrated suspensions (83,86–89), and of viscoelastic properties (90–92).

The viscosities of dilute dispersions have received considerable theoretical and experimental treatment, partly because of the similarity between polymer solutions and small particle dispersions at low concentration. Nondeformable spherical particles are usually assumed in the cases of molecules and particles. The key viscosity quantity for dispersions is the relative viscosity or viscosity ratio, η_{rel}.

$$\eta_{\text{rel}} = \frac{\eta}{\eta_0} = \frac{\text{Dispersion viscosity}}{\text{Viscosity of liquid}} \tag{9}$$

This is because the effect of the dispersed solid, rather than the dispersing medium, is usually more significant. However, the latter should not be ignored. Many industrial problems involving unacceptably high viscosities in dispersed systems are solved by substituting solvents of lower viscosity.

The relative viscosity of a dilute dispersion of rigid spherical particles is given by $\eta_{\text{rel}} = 1 + a\phi$, where a is equal to $[\eta]$, the limiting viscosity number (intrinsic viscosity) in terms of volume concentration, and ϕ is the volume fraction. Einstein has shown that, provided that the particle concentration is low enough and certain other conditions are met, $[\eta] = 2.5$, and the viscosity equation is then $\eta_{\text{rel}} = 1 + 2.5\phi$. This expression is usually called the Einstein equation.

For higher ($\phi > 0.05$) concentrations where particle–particle interactions are noticeable, the viscosity is higher than that predicted by the Einstein equation. The viscosity–concentration equation becomes equation 14, where b and c are additional constants (93).

$$\eta_{\text{rel}} = 1 + 2.5\phi + b\phi^2 + c\phi^3 + \cdots \tag{10}$$

The deviation from the Einstein equation at higher concentrations is represented in Figure 9, which is typical of many systems (94,95). The relative viscosity tends to infinity as the concentration approaches the limiting volume fraction of close packing ϕ_m ($\phi = \sim 0.7$). Equation 14 has been modified (96,97) to take this into account, and the expression for η_{rel} becomes (eq. 11)

$$\eta_{\text{rel}} = \frac{1 + 2.5\phi + b\phi^2 + c\phi^3 + \cdots}{1 - (\phi_{\text{m}}/\phi)} \tag{11}$$

Another model that has been successful in fitting much data is the Krieger–Dougherty equation (eq. 16) (8,98):

$$\eta_{\mathrm{rel}} = \left(1 - \frac{\phi}{\phi_{\mathrm{m}}}\right)^{-[\eta]\phi_{\mathrm{m}}}$$

Factors other than concentration affect the viscosity of dispersions. A dispersion of nonspherical particles tends to be more viscous than predicted if the Brownian motion is great enough to maintain a random orientation of the particles. However, at low temperatures or high solvent viscosities, the Brownian motion is small and the particle alignment in flow (streamlining) results in unexpectedly lower viscosities. This is a form of shear thinning.

If the dispersion particles are attracted to each other, they tend to flocculate and form a structure. At low concentrations the particles form open aggregates, which give a fractal structure (99,100). At higher concentrations a network structure results, which can be so pronounced that the mixture has a yield point and behaves like a solid when at rest. Shearing breaks up this structure, and viscosity decreases.

If the volume concentration of the solid in the dispersion is high enough, shearing may produce an increase rather than a decrease in viscosity. Such behavior, called *shear thickening* (8,16,101,102) or *dilatancy*, is common in dispersions of certain pigments and other powders. These dispersions are closely packed, but are usually shear thinning up to moderate shear rates, ie, a few hundred to a few thousand per second. Higher shear introduces irregularities in the packing, with bridging effects occurring between the particles. The overall packing loosens, which implies that the total space between particles increases. The liquid is not able to fill this space and can no longer wet all the particles. Much of the lubricating effect of the liquid is therefore lost, and internal friction rises, producing a high viscosity. This is true dilatancy, and the volume actually increases. Shear thickening can also occur in dilute suspensions (103). In such cases there is no volume expansion; instead there is buildup of particle aggregates which ultimately produces a network that behaves like a gel.

Because emulsions are different from dispersions, different viscosity–concentration relationships must be used (76,93). In an emulsion the droplets are not rigid, and viscosity can vary over a wide range. Several equations have been proposed to account for this. An extension of the Einstein equation includes a factor that allows for the effect of variations in fluid circulation within the droplets and subsequent distortion of flow patterns (104,105).

2.8. Extensional Viscosity. In addition to the shear viscosity η, two other rheological constants can be defined for fluids: the bulk viscosity, K, and the extensional or elongational viscosity, η_{e} (36,50,51,106–110). The bulk viscosity relates the hydrostatic pressure to the rate of deformation of volume, whereas the extensional viscosity relates the tensile stress to the rate of extensional deformation of the fluid. Extensional viscosity is important in a number of industrial processes and problems (36,106,111,112). Shear properties alone are insufficient for the characterization of many fluids, particularly polymer melts (107,110,113,114).

Extensional flows occur when fluid deformation is the result of a stretching motion. Extensional viscosity is related to the stress required for the stretching. This stress is necessary to increase the normalized distance between two

material entities in the same plane when the separation is s and the relative velocity is ds/dt. The deformation rate is the extensional strain rate, which is given by equation 17(111):

$$\dot{\varepsilon} = \frac{1}{s}\frac{ds}{dt} \tag{13}$$

Unlike shear viscosity, extensional viscosity has no meaning unless the type of deformation is specified. The three types of extensional viscosity identified and measured are uniaxial or simple, biaxial, and pure shear. Uniaxial viscosity is the only one used to characterize fluids. It has been employed mainly in the study of polymer melts, but also for other fluids. For a Newtonian fluid, the uniaxial extensional viscosity is three times the shear viscosity: $(\eta_e)_{uni} = 3\eta$. The two other extensional viscosities are used to study elastomers in the form of films or sheets. Uniaxial and biaxial extensions are important in industry (106,110–112,114,115), the former for the spinning of textile fibers and roller spattering of paints, and the latter for blow molding, vacuum forming, film blowing, and foam processes.

2.9. Electrorheological Behavior. Electrorheological (ER) fluids are colloidal suspensions whose properties change strongly and reversibly upon application of an electric field. When an electric field is applied to an ER fluid, it responds by forming fibrous or chain structures parallel to the applied field. These structures greatly increase the viscosity of the fluid, by a factor of 10^5 in some cases. At low shear stress the material behaves like a solid. The material has a yield stress, above which it will flow, but with a high viscosity.

A parameter used to characterize ER fluids is the Mason number, M_a, which describes the ratio of viscous to electrical forces, and is given by equation 18, where ε is the solvent dielectric constant; η_0, the solvent viscosity; $\gamma\cdot$, the strain or shear rate; β, the effective polarizability of the particles; and E, the electric field (116).

$$M_a = \frac{24\pi\varepsilon\eta_0\dot{\gamma}}{(\beta E)^2} \tag{14}$$

A considerable literature on ER fluids and their measurement has developed: a selection of reviews and papers is given in References (117–138). There is an analogous magnetorheological (MR) effect where suspensions filled with magnetic particles show reversible changes in their rheological behavior when subjected to a magnetic field (138–143). Measurements on ER and MR fluids are made with viscometers modified to allow the the application of electric or magnetic fields.

3. Elasticity and Viscoelasticity

Elastic deformation is a function of stress and is expressed in terms of relative displacement or strain. Strain may be expressed in terms of relative change in volume, length, or other measurement, depending on the nature of the stress. An ideal elastic body (144,145) is a material for which the strain is proportional to the stress (Hooke's law) with immediate recovery to the original volume and shape when the stress is released. The relationship between the stress σ and strain ε may be written as $\sigma = K\varepsilon$, where K is a proportionality constant called the modulus of elasticity. For a homogeneous, isotropic, Hookean solid, three moduli may be defined. Young's modulus, E, relates tensile stress to tensile strain. The shear modulus, G, relates shear stress to shear strain, ie, $G = \tau/\gamma$. The bulk modulus B relates hydrostatic pressure to the change in volume. Another elastic constant needed for complete specification of behavior in tension is Poisson's ratio, μ, which relates change in volume to change in shape. Incompressible solids and polymer melts have $\mu = 0.5$, but for most solid materials, $\mu < 0.5$. For isotropic, Hookean materials, Young's modulus is related to the shear modulus by $E = 2G(1 + \mu)$. If μ is 0.5, Young's modulus is three times the shear modulus. Values for the various moduli and Poisson's ratio for some representative materials are given in Table 3.

Materials such as metals are nearly elastic and show almost no flow or viscous component. Polymers and many of their solutions are both viscous and elastic, and both types of deformation must be taken into account to explain their behavior (see Viscoelasticity).

3.1. Mechanical Behavior of Materials. Different kinds of materials respond differently when they undergo mechanical stress. For purely viscous behavior, stress is relieved by viscous flow and is independent of strain. For purely elastic behavior, there is a direct dependence of stress on strain and the ratio of the two is the modulus E (or G).

The response of different materials to a constant stress applied at time $t = t_0$ followed by removal of that stress at $t = t_1$, ie, creep and recovery, is shown in Figure 10 (146). For an elastic material (Fig. 10**a**), the resulting strain is instantaneous and constant until the stress is removed, at which time the material recovers and the strain immediately drops back to zero. In the case of the viscous fluid (Fig. 10**b**), the strain increases linearly with time. When the load is removed, the strain does not recover but remains constant. Deformation is permanent. The response of the viscoelastic material (Fig. 10**c**) draws from both kinds of behavior. An initial instantaneous (elastic) strain is followed by a time-dependent strain. When the stress is removed, the initial strain recovery is elastic, but full recovery is delayed to longer times by the viscous component.

3.2. Mechanical Models. Because the complex rheological behavior of viscoelastic bodies is difficult to visualize, mechanical models are often used. In these models the viscous response to applied stress is assumed to be that of a Newtonian fluid and is represented by a dashpot, ie, a piston operating in a cylinder of Newtonian fluid. The elastic response is idealized as an ideal elastic (Hookean) solid and is represented by a spring. The dashpot represents the dissipation of energy in the form of heat, whereas the spring represents a system

that stores energy. Mechanical behavior of materials may be approximated by combinations of springs and dashpots. These models, which are largely being replaced by mathematical (integral and differential) models, have been covered in detail elsewhere (8,10,20,93,146,147).

Whether a viscoelastic material behaves as a viscous liquid or an elastic solid depends on the relation between the time scale of the experiment and the time required for the system to respond to stress or deformation. Although the concept of a single relaxation time is generally inapplicable to real materials, a *mean characteristic time* can be defined as the time required for a stress to decay to $1/e$ of its elastic response to a step change in strain. The ratio of this characteristic time to the time scale of the experiment, t_e, is called the Deborah number. A material at a high Deborah number responds elastically, whereas that at a low Deborah number exhibits viscous behavior: at $t_e - \lambda$, it behaves like an elastic solid; at 0 $t_e > \lambda$, like a viscous liquid. These effects can be seen in geological strata, where rock has flowed to relieve the stresses imposed by geological events. The time scale is long, and the material appears to be viscous.

3.3. Dynamic Behavior. Knowledge of the response of materials to stress–strain, creep, and stress–relaxation measurements are useful to define material properties. The dynamic response of viscoelastic materials to cyclic stresses or strains is also important, partly because cyclic motion occurs in many processing operations and applications, and partly because so much rheological information can be gained from dynamic measurements. By subjecting a specimen to oscillatory stress and determining the response, both the elastic and viscous or damping characteristics can be obtained. Elastic materials store energy, whereas liquids dissipate it as heat. This dissipation results in highly damped motion. Viscoelastic materials exhibit both elastic and damping behavior. The latter causes the deformation to be out of phase with the stress applied in the dynamic measurement.

A sinusoidal stress applied to an ideal elastic material produces a sinusoidal strain proportional to the stress amplitude and in phase with it. For ideal viscous materials the stress and strain are out of phase by 90°. Figure 11 gives an example of a stress–strain diagram for a sinusoidal stress applied to a real material. The amplitude of the deformation (strain) in response to the stress is proportional to that of the stress, but lags behind the strain curve by some angle δ between 0 and 90°, depending on the elastic/viscous characteristic of the material. This behavior is usually analyzed by the use of complex variables to represent stress and strain. These variables, complex stress and complex strain, ie, τ^* and γ^*, respectively, are vectors in complex planes. They can be resolved into real (in phase) and imaginary (90° out of phase) components.

The complex stress is $\tau^* = \tau' + i\tau''$, which is the sum of a real part of the stress and an imaginary part; the complex strain is $\gamma^* = \gamma' + i\gamma''$, where i is the operator $\sqrt{-1}$ that signifies the rotation of 90° between τ' and τ' and γ' and γ''. The shear modulus can also be represented by a complex variable, ie, the complex dynamic modulus G^*, which is the ratio of the complex stress and complex strain: $G^* = \tau^*/\gamma^*$. The dynamic modulus can also be resolved into two components or vectors (G' and G''): $G^* = G' + iG''$, where equation 15 holds, and where $G' = G^* \cos \delta$ and $G'' = G^* \sin \delta$.

$$G^* = [(G')^2 + (G'')^2]^{-1} \tag{15}$$

The parameter G' is called the storage modulus. It is in phase with the real components of γ^* and τ^* and is a measure of elasticity. It is associated with the energy stored in elastic deformation and is approximately equal to the elastic modulus determined in creep and stress–relaxation experiments when measured at appropriate timescales, ie, $G'(\omega)G(t)$ when $t = 1/\omega$. The value of G' is high when a polymer is in its glassy state, but drops with increasing temperature as the polymer goes through the glass transition and becomes soft and rubbery (Fig. 12). If the polymer is cross-linked, the storage modulus does not drop so far after the glass transition. The exact level depends on the degree of cross-linking. For viscoelastic melts it is common practice to associate G' with the ability of a melt to recover from a deformation. However, this has been shown to be invalid in some cases, and an association with the stiffness of the melt is preferred (148).

G'' is called the loss modulus. It arises from the out-of-phase components of γ^* and τ^* and is associated with viscous energy dissipation, ie, damping. The ratio of G'' and G' gives another measure of damping, the dissipation factor or loss tangent (often just called tan δ), which is the ratio of energy dissipated to energy stored (eq. 16).

$$\tan \delta = G''/G' \tag{16}$$

Plots of loss modulus or tan δ vs temperature for polymers give peaks at energy absorbing transitions, such as the glass transition and low temperature secondary transitions (Fig. 13). Such plots are useful for characterizing polymers and products made from them.

A viscoelastic material also possesses a complex dynamic viscosity, $\eta^* = \eta' + i\eta''$, and it can be shown that $\eta^* = G^*/i\omega$; $\eta' = G''/\omega$; and $\eta'' = G'/\omega$, where ω is the angular frequency. The parameter η^* is useful for many viscoelastic fluids in that a plot of its absolute value η^* vs angular frequency in rad/s is often numerically similar to a plot of shear viscosity η vs shear rate. This correspondence is known as the Cox–Merz empirical relationship (150,151). The parameter η' is called the dynamic viscosity and is related to G'', the loss modulus; the parameter η'' does not deal with viscosity, but is a measure of elasticity.

The significance of G'', G', tan δ, η', and η'' is that they can be determined experimentally and used to characterize real materials. These parameters depend on frequency and temperature, and this dependence can be used to define behavior. For example, viscoelastic fluids are often characterized by log–log plots of one or more of these quantities vs the angular frequency ω, as shown in Figure 14, which illustrates the behavior of a polymer melt (152,153).

3.4. Normal Stress (Weissenberg Effect). Many viscoelastic fluids flow in a direction normal (perpendicular) to the direction of shear stress in steady-state shear (20,96). Examples of the effect include flour dough climbing up a beater, polymer solutions climbing up the inner cylinder in a concentric cylinder viscometer, and paints forcing apart the cone and plate of a cone–plate viscometer. The normal stress effect has been put to practical use in certain screwless extruders designed in a cone–plate or plate–plate configuration, where the polymer enters at the periphery and exits at the axis.

The two normal stress functions, $N_1(\gamma\cdot)$ and N_2 $(\gamma\cdot)$, are referred to as the first and second normal stress differences, respectively. The former is positive and increases with increasing shear rate, as shown in Figure 15 (152,153), which describes the steady-shear behavior of the polymer melt in Figure 14. The stress function N_2 $(\gamma\cdot)$ is smaller in absolute value than $N_1(\gamma\cdot)$ and is sometimes negative. The first normal stress difference is a useful quantity, as it often gives a good quantitative measure of viscoelasticity. It can be determined from the normal force, which is measurable with several commercial rotational viscometers. In highly elastic liquids it is common for $N_1(\gamma\cdot)$ to be considerably larger than the shear stress.

Description of normal stress measurements on a practical but complex material, paint, is available (154). Other publications (155–158) give the results of investigations of normal stress differences for a variety of materials. These papers and their references form a useful introduction to the measurement of normal stress differences.

4. Viscometers

To solve a flow problem or characterize a given fluid, an instrument must be carefully selected. Many commercial viscometers are available with a variety of geometries for wide viscosity ranges and shear rates (8,20,47,51). Rarely is it necessary to construct an instrument. However, in choosing a commercial viscometer a number of criteria must be considered. Of great importance is the nature of the material to be tested, its viscosity, its elasticity, the temperature dependence of its viscosity, and other variables. The degree of accuracy and precision required, and whether the measurements are for quality control or research, must be considered. The viscometer must be matched to the materials and processes of interest; otherwise, the results may be misleading.

Most early viscometers, many of which have been incorporated into standard industrial tests, give single-point measurements. Instead of describing viscosity or shear stress over a range of shear rates, only a single point on the flow curve is produced; the rest of the curve is unknown. This is not a problem with Newtonian liquids because viscosity is independent of shear rate, but it can be misleading in the case of non-Newtonian materials, as shown in Figure 16, where the viscosity profiles of two fluids cross each other. Measurements carried out at the shear rate corresponding to the intersection would indicate that the two materials are identical, even though a simple examination, such as shaking or pouring, would show that they are not. A non-Newtonian fluid cannot be adequately characterized by a single-point measurement, and multipoint measurement techniques are strongly recommended.

Temperature control is also important. Viscosity is highly dependent on temperature; accurate, precise measurements can be made only if the temperature is carefully controlled. More errors are made and more disagreements over viscosity results arise because of incorrect or drifting temperature than for any other reason. Good temperature control can be achieved with commercial baths or circulators equipped with thermostats. Unfortunately, this is impossible with some viscometers. Others lose temperature control because of heat generation at

high shear rates, especially with high viscosity materials. Such a temperature increase causes an apparent loss of viscosity under shear. A natural but erroneous conclusion would be that the material is thixotropic or shear thinning.

Viscometers may be separated into three main types: capillary, rotational, and moving body. There are other kinds, usually designed for special applications. For example, it has been reported that the viscosity of volumes of liquid in the nanoliter range can be measured by monitoring the shape of a droplet while it is suspended in a medium with an extensional or shear field (159). For any given type of viscometer there is usually a choice of several different instruments. The choice depends on the particular requirements of the investigator and the price range.

4.1. Capillary Viscometers. Capillary flow measurement is a popular method for measuring viscosity (20,146,147); it is also the oldest. A liquid drains or is forced through a fine-bore tube, and the viscosity is determined from the measured flow, applied pressure, and tube dimensions. The basic equation is the Hagen–Poiseuille expression (eq. 17), where η is the viscosity, r the radius of the capillary, Δp the pressure drop through the capillary, V the volume of liquid that flows in time t, and L the length of the capillary.

$$\eta = \frac{\pi r^4 \Delta p t}{8VL} \tag{17}$$

Steady-state, laminar, isothermal flow is assumed. For a given viscometer with similar fluids and a constant pressure drop, the equation reduces to $\eta = Kt$ or, more commonly, $\nu = \eta/\rho = Ct$, where ρ is the density, ν the kinematic viscosity, and C a constant. Therefore, viscosity can be determined by multiplying the efflux time by a suitable constant.

Capillary viscometers are useful for measuring precise viscosities of a large number of fluids, ranging from dilute polymer solutions to polymer melts. Shear rates vary widely and depend on the instruments and the liquid being studied. The shear rate at the capillary wall for a Newtonian fluid may be calculated from equation 18, where Q is the volumetric flow rate and r the radius of the capillary; the shear stress at the wall is $\tau_w = r\Delta p/2L$.

$$\dot{\gamma}_w = \frac{4Q\pi}{r^3} \tag{18}$$

Absolute viscosities are difficult to measure with capillary viscometers, but viscosities relative to some standard fluid of known viscosity, such as water, are readily determined. The viscometer is calibrated with the reference fluid, and viscosities of other fluids relative to the reference sample are determined from their flow times.

For highly accurate work, corrections must be made for kinetic energy losses, incomplete drainage, turbulence, and possible surface tension and heat effects (20). The largest correction for liquids is that resulting from loss of effective pressure because of the appreciable kinetic energy of the issuing stream. The next most important correction for liquids and the largest for polymer melts is

that for energy loss resulting from end effects, ie, viscous resistance caused by velocity gradients as the liquid enters and leaves the capillary (146,147,160). When the terms for these two correction factors are incorporated into the viscosity equation, it is changed to equation 19, where t is the time of flow and B and C are instrument constants generated from measurements of fluids of known viscosity.

$$\nu = \eta/\rho = Ct - B/t \tag{19}$$

These corrections are rarely used in industrial applications because the Poiseuille equation adequately expresses the flow. However, corrections are absolutely necessary for determining even approximate viscosities when using short capillary devices, such as orifice viscometers. Use of a long capillary ($>$ 10 dia) and long efflux times ($>$ 300 s) minimizes the need for corrections. The ASTM standards D3835 and D5099 describe experimental procedures for using capillary rheometers to measure rheological properties of polymers and rubbers under process conditions.

The glass capillary viscometer is widely used to measure the viscosity of Newtonian fluids. The driving force is usually the hydrostatic head of the test liquid. Kinematic viscosity is measured directly, and most of the viscometers are limited to low viscosity fluids, approx 0.4–16,000 mm^2/s. However, external pressure can be applied to many glass viscometers to increase the range of measurement and enable the study of non-Newtonian behavior. Glass capillary viscometers are low shear stress instruments: 1–15 Pa or 10–150 dyn/cm^2 if operated by gravity only. The rate of shear can be as high as 20,000 s^{-1} based on a 200–800 s efflux time.

The basic design is that of the Ostwald viscometer: a U-tube with two reservoir bulbs separated by a capillary, as shown in Figure 17**a**. The liquid is added to the viscometer, pulled into the upper reservoir by suction, and then allowed to drain by gravity back into the lower reservoir. The time that it takes for the liquid to pass between two etched marks, one above and one below the upper reservoir, is a measure of the viscosity. In U-tube viscometers, the effective pressure head and therefore the flow time depend on the volume of liquid in the instrument. Hence, the conditions must be the same for each measurement.

The original Ostwald viscometer has been modified in many ways, and a number of different versions are on the market (20). Most are available with a wide choice of capillary diameters and therefore a number of viscosity ranges. A number of viscometers are described in ASTM D445, which also lists detailed recommendations on dimensions and methods of use.

The Cannon–Fenske viscometer (Fig. 17**b**) is excellent for general use. A long capillary and small upper reservoir result in a small kinetic energy correction; the large diameter of the lower reservoir minimizes head errors. Because the upper and lower bulbs lie on the same vertical axis, variations in the head are minimal even if the viscometer is used in positions that are not perfectly vertical. A reverse-flow Cannon–Fenske viscometer is used for opaque liquids. In this type of viscometer the liquid flows upward past the timing marks, rather

than downward as in the normal direct-flow instrument. Thus the position of the meniscus is not obscured by the film of liquid on the glass wall.

The Ubbelohde viscometer is shown in Figure 17**c**. It is particularly useful for measurements at several different concentrations, as flow times are not a function of volume, and therefore dilutions can be made in the viscometer. Modifications include the Cannon-Ubbelohde, semi-micro, and dilution viscometers. The Ubbelohde viscometer is also called a suspended-level viscometer because the liquid emerging from the lower end of the capillary flows down only the walls of the reservoir directly below it. Therefore, the lower liquid level always coincides with the lower end of the capillary, and the volume initially added to the instrument need not be precisely measured. This also eliminates the temperature correction for glass expansion necessary for Cannon–Fenske viscometers.

For accurate and precise measurement the glass capillary must be clean. The viscometer must be cleaned thoroughly after each series of operations. Samples being tested and cleaning solvents should be filtered to remove particles that can clog the capillary.

All glass capillary viscometers should be calibrated carefully (20). The standard method is to determine the efflux time of distilled water at 20°C. Unfortunately, because of its low viscosity, water can be used only to standardize small capillary instruments. However, a calibrated viscometer can be used to determine the viscosity of a higher viscosity liquid, such as a mineral oil. This oil can then be used to calibrate a viscometer with a larger capillary. Another method is to calibrate directly with two or more certified standard oils differing in viscosity by a factor of approximately 5. Such oils are useful for calibrating virtually all types of viscometers. Because viscosity is temperature-dependent, particularly in the case of standard oils, temperature control must be extremely good for accurate calibration.

In recent years several commercial capillary viscometers that allow automation have been developed. Manufacturers of automated viscosity systems include Cannon, Schott, Design Scientific, and Lauda; Wescan supplies timer and photocell combinations. An inexpensive timer is based on light pipes and an electronic stopwatch (161). Cannon Instrument Co. supplies a wide range of glass capillary viscometers, temperature baths, viscosity standards, and related equipment.

Orifice viscometers, also called efflux or cup viscometers, are commonly used to measure and control flow properties in the manufacture, processing, and application of inks, paints, adhesives, and lubricating oils. Their design answered the need for simple, easy-to-operate viscometers in areas where precision and accuracy are not particularly important. In these situations knowledge of a true viscosity is unnecessary, and the efflux time of a fixed volume of liquid is a sufficient indication of the fluidity of the material. Examples of orifice viscometers include the Ford, Zahn, and Shell cups used for paints and inks and the Saybolt Universal and Furol instruments used for oils.

Orifice viscometers usually have extremely short capillaries. The typical orifice viscometer is a cup with a hole in the bottom. The cup is filled, and the time required for the liquid to flow out is measured. The hydrostatic head decreases as the liquid flows, and there is a large kinetic energy effect. Flow

analysis shows that the flow does not follow the Hagen–Poiseuille law, and efflux times are not related to viscosities in any simple manner. Therefore, it is better not to convert efflux times to viscosities except during calibration with standard oils. Efflux times should be accepted as arbitrary measures of viscosity and noted in terms of the viscometer being used, ie, Saybolt seconds, Ford seconds, etc. The precision of orifice viscometers is poor because of the lack of temperature control, wear during use, and variations in manufacture. However, they are widely used in industry because they are inexpensive, robust, and easy to use. Some of these instruments have the added convenience of being capable of dipping into or remaining in the material to be tested. Dip cups determine approximate or relative viscosities in resin reactors, ink reservoirs, paint dip tanks, adhesive mixing tanks, etc. These are applications where the limitations of orifice cups are unimportant.

Orifice viscometers should not be used for setting product specifications, for which better precision is required. Because they are designed for Newtonian and near-Newtonian fluids, they should not be used with thixotropic or highly shear-thinning materials; such fluids should be characterized by using multispeed rotational viscometers.

Some orifice viscometers, such as the Shell dip cup and the European ISO cup, which resembles a Ford cup with a capillary, have long capillaries. These cups need smaller kinetic energy corrections and give better precision than the corresponding short-capillary viscometers. However, they are still not precision instruments, and should be used only for control purposes.

If it is necessary to calculate kinematic viscosities from efflux times, such as in a calibration procedure, equation 20 should be used, where t is the efflux time and k and K are constants characteristic of the particular viscosity cup (162–165).

$$\nu = kt - K/t$$

In most cases it is sufficient to be able to convert from one viscometer value to another or to approximate kinematic viscosities with the help of charts or tables; literature from manufacturers is useful.

Linear equations of the type $\nu = ct - C$, where c and C are constants, relate kinematic viscosity to efflux time over limited time ranges. This is based on the fact that, for many viscometers, portions of the viscosity–time curves can be taken as straight lines over moderate time ranges. Linear equations, which are simpler to use in determining and applying correction factors after calibration, must be applied carefully as they do not represent the true viscosity–time relation. Linear equation constants have been given (162) and are used in ASTM D4212.

Pressure-driven piston cylinder capillary viscometers, ie, extrusion rheometers (Fig. 18), are used primarily to measure the melt viscosity of polymers and other viscous materials (20,47,49,51). A reservoir is connected to a capillary tube, and molten polymer or another material is extruded through the capillary by means of a piston to which a constant force is applied. Viscosity can be determined from the volumetric flow rate and the pressure drop along the capillary.

The basic method and test conditions for a number of thermoplastics are described in ASTM D1238. Melt viscoelasticity can influence the results (171).

Polymer melts are frequently non-Newtonian. In this case the earlier expression given for the shear rate at the capillary wall does not hold. A correction factor $(3n+1)/4n$, called the Rabinowitsch correction, must be applied in such a way that equation 21 applies, where $\gamma_{\cdot tw}$ is the true shear rate at the wall and n is a power law factor (eq. 22) determined from the slope of a log–log plot of the true shear stress at the wall, τ_{tw}, vs $\gamma_{\cdot w}$. For a Newtonian liquid, $n=1$. A true apparent viscosity, η_t, can be calculated from equation 23.

$$\dot{\gamma}_w = \frac{(3n+1)\dot{\gamma}_w}{4n} \tag{21}$$

$$n = \frac{d\log \tau_{tw}}{d\log \dot{\gamma}_w} \tag{22}$$

$$\eta_t = \frac{\tau_{tw}}{\dot{\gamma}_{tw}} \tag{23}$$

An even more important correction for polymer melts is that for end effects. Entrance and exit effects cause pressure drops that interfere with an accurate determination of the pressure gradient, $\Delta p/L$, needed for viscosity determination using the Hagen–Poiseuille equation. It has been assumed (160) that the effective length of the capillary is greater than the actual length, and the shear stress at the wall has been corrected as equation 24, where R is the capillary radius, L is the actual length, and E is an empirical parameter obtained by extrapolating a plot of Δp versus the capillary aspect ratio, L/R, to zero pressure drop at constant shear rate, $\dot{\gamma}$, for capillaries of different length (146).

$$\tau_w^c = \frac{R\Delta p}{2(L+ER)} \tag{24}$$

A number of instruments are based on the extrusion principle, including slit flow and normal capillary flow. These instruments are useful when large numbers of quality control or other melt viscosity test measurements are needed for batches of a single material or similar materials. When melt viscosities of a wide range of materials must be measured, rotational viscometers are preferable. Extrusion rheometers have been applied to other materials with some success with adhesives and coatings (8).

4.2. Rotational Viscometers. Rotational viscometers consist of two basic parts separated by the fluid being tested (20,146,147,162,165–170). The parts may be concentric cylinders (cup and bob), plates, a low angle cone and a plate, or a disk, paddle, or rotor in a cylinder. Rotation of one part against the other produces a shearing action on the fluid. The torque required to produce a given angular velocity or the angular velocity resulting from a given torque is a measure of the viscosity. Rotational viscometers are more versatile than capillary viscometers. They can be used with a wide range of materials because opacity, settling, and non-Newtonian behavior do not cause difficulties. Viscosities over a range of shear rates and as a function of time can be measured.

Therefore, they are useful for characterizing shear thinning and time-dependent behavior.

Since the 1990s rotational viscometers have been developed that have integrated computers for operation and control of the instrument as well as for data collection, reduction, and storage. The combination of a computer, modern electronics, and feedback loops provides great flexibility and control. For example, pulses from the computer coupled with feedback from the viscometer can give precise oscillatory motion as well as shear viscosity measurement at constant stress or speed; only simple hardware is involved. Such instruments are useful for rheological measurements and studying the structure of dispersions and formulated products. These new instruments are versatile, easy to use, and allow the collection, analysis, and comparison of large amounts of data in a short time.

The mechanical parts of computer-controlled viscometers can be simple and should not become obsolete for many years. The complexity is in the software, and this is where changes will have to be made to keep the instrument up to date. Some manufacturers are offering new, updated software free for a period of several years after the instrument is purchased.

Rotational viscometers often were not considered for highly accurate measurements because of problems with gap and end effects. However, corrections can be made, and very accurate measurements are possible. Operating under steady-state conditions, they can closely approximate industrial process conditions such as stirring, dispersing, pumping, and metering. They are widely used for routine evaluations and quality control measurements. The commercial instruments are effective over a wide range of viscosities and shear rates.

The equations and methods for determining viscosity vary greatly with the type of instrument, but in many cases calculations may be greatly simplified by calibration of the viscometer with a standard fluid, the viscosity of which is known for the conditions involved. General procedures for calibration measurement are given in ASTM D2196. The constant thus obtained is used with stress and shear rate terms to determine viscosity by equation 25, where the stress term may be torque, load, or deflection, and the shear rate may be in rpm, revolutions per second (rps), or s^{-1}.

$$\eta = K(\text{stress term/shear rate term}) \tag{25}$$

Constants and factors are often supplied by the manufacturer. Separate constants may be given for converting the stress and shear rate terms to the correct quantities and units.

A constant is often determined from measurements with a Newtonian oil, particularly when the calibrations are supplied by the manufacturer. This constant is valid only for Newtonian specimens; if used with non-Newtonian fluids, it gives a viscosity based on an inaccurate shear rate. However, for relative measurements this value can be useful. Employment of an instrument constant can save a great deal of time and effort and increase accuracy because end and edge effects, slippage, turbulent interferences, etc, are included.

The earliest and probably the most common type of rotational viscometer is the coaxial or concentric cylinder instrument. It consists of two cylinders, one

within the other (cup and bob), keeping the specimen between them, as shown in Figure 19. The first practical rotational viscometer consisted of a rotating cup with an inner cylinder supported by a torsion wire. In variations of this design the inner cylinder rotates. Instruments of both types are useful for a variety of applications.

The relationship between viscosity, angular velocity, and torque for a Newtonian fluid in a concentric cylinder viscometer is given by the Margules equation (eq. 26) (20,147), where M is the torque on the inner cylinder, h the length of the inner cylinder, Ω the relative angular velocity of the cylinder in radians per second, R_i the radius of the inner cylinder wall, R_o the radius of the outer cylinder wall, and k an instrument constant.

$$\eta = \left(\frac{M}{\Omega 4\pi h}\right)\left(\frac{1}{R_i^2} - \frac{1}{R_o^2}\right) = \frac{kM}{\Omega} \tag{26}$$

Therefore, the viscosity can be determined from the torque and angular velocity. However, the viscosity is usually calculated from the shear rate and shear stress, which can be obtained from the Margules equation. The shear rate is given by equation 27, where r is any given radius.

$$\dot{\gamma} = \frac{(2\Omega/r^2)(R_i^2 R_o^2)}{R_o^2 - R_i^2} \tag{27}$$

The shear stress is given by equation 28:

$$\tau = \frac{M}{2\pi r^2 h} \tag{28}$$

The shear rate and shear stress can be calculated for any radius r from these equations. In most cases the radius used is R_i because the shear stress and shear rate of interest are at the inner, torque-sensing cylinder. Thus equations 27 and 28 become

$$\dot{\gamma} = \frac{2\Omega R_o^2}{R_o^2 - R_i^2} \text{ and } \tau = \frac{M}{2\pi R_i^2 h}$$

The viscosity of a Newtonian fluid may be determined from the Margules equation or from the slope of a shear stress–shear rate plot. Non-Newtonian fluids give intercepts and curves with such plots. Viscosities can be calculated, but accurate values depend on including correction factors for yield points and shear thinning, ie, shear rate corrections, in the above equations (20). The shear rate correction may be minimized by using a very small gap size; in other words, the ratio of the inner to outer radius should be as close to unity as possible. In practical terms this means maintaining a ratio of 0.95, which is impossible with many sensors used with commercial rotational viscometers. With highly shear thinning materials even this is insufficient, and corrections

must be made regardless of the gap size. However, with viscosity–shear rate curves, although correction shifts each point by a rather large amount, the corrected curve itself is only slightly different from the uncorrected curve (172).

In addition to non-Newtonian flow, the main correction necessary for concentric cylinder measurements is that on account of end effects. Because the inner cylinder is not infinitely long, there is drag on the ends as well as on the face of the cylinder. The correction appears as an addition, h_0, to the length, h. The correction is best determined by measuring the angular velocity and torque at several values of h, that is, at various depths of immersion. The data are plotted as M/Ω vs h, and extrapolation is made to a value of h_0 at $M/\Omega = 0$. The quantity $(h + h_0)$ is substituted for h in the various equations.

In a cone–plate viscometer (Fig. 20), a low angle ($\leq 3^\circ$) cone rotates against a flat plate with the fluid sample between them. The cone–plate instrument is a simple, straightforward device that is easy to use and extremely easy to clean. It is well-suited to routine work because measurements are rapid and no tedious calculations are necessary. With careful calibration and good temperature control it can be a very effective research and problem-solving tool. Heated instruments can be used for melt viscosity measurements.

In most rotational viscometers the rate of shear varies with the distance from a wall or the axis of rotation. However, in a cone–plate viscometer the rate of shear across the conical gap is essentially constant because the linear velocity and the gap between the cone and the plate both increase with increasing distance from the axis. No tedious correction calculations are required for non-Newtonian fluids. The relevant equations for viscosity, shear stress, and shear rate at small angles α of fluids are equations 29, 30, and 31, respectively, where M is the torque, R_c the radius of the cone, v the linear velocity, and r the distance from the axis.

$$\eta = \frac{3\alpha M}{2R_c^3} \tag{29}$$

$$\tau = \frac{3M}{2\pi R_c^3} \tag{30}$$

$$\dot{\gamma} = \frac{d\nu}{dr} = \frac{\Omega}{\alpha} \tag{31}$$

Cone–plate geometry has several advantages over concentric cylinder geometry, including a smaller sample size, a homogeneous shear rate, and easy conversion of data. Disadvantages include the need for precise adjustment of the gap (done automatically in many viscometers), including resetting when the temperature is changed, specimen drying, solvent evaporation, slinging of material from the gap, and the possibility of viscous heating, particularly at high shear rates. The last problem is compounded by the fact that temperature control with commercial instruments is not always as good as it should be.

In parallel plate viscometers (168) the gap width is usually larger and can be varied freely. This is an advantage when measuring suspensions or dispersions with large particles or with a tendency to fly out of the gap. The wide gap means that there is less sensitivity to temperature changes. Therefore, reset-

ting is usually not necessary and temperature scans are much easier to run than with a cone–plate viscometer. However, with the plate–plate instrument, the velocity, and therefore the shear rate, varies with the distance from the center of the plate. This makes viscosity data more difficult to evaluate.

The maximum shear rate (at the plate rim) is given by equation 32, where R_p is the radius of the plate and h the distance between the two plates.

$$\dot{\gamma}_m = \frac{\Omega R_p}{h} \tag{32}$$

The viscosity is given by equation 33, where M is the torque.

$$\eta = \frac{3M}{2\pi R_p^3 \dot{\gamma} m}\left(1 + 3\frac{d\ln M}{d\ln \dot{\gamma}}\right) \tag{33}$$

A dynamic viscometer is a special type of rotational viscometer used for characterizing viscoelastic fluids. It measures elastic as well as viscous behavior by determining the response to both steady-state and oscillatory shear. The geometry may be cone–plate, parallel plates, or concentric cylinders; parallel plates have several advantages, as noted above.

Many rotational viscometers operate by controlling the rotational speed and, therefore, the shear rate. The shear stress varies uncontrollably as the viscosity changes. Often, before the structure is determined by viscosity measurement, it is destroyed by the shearing action. Yield behavior is difficult to measure. In addition, many flow processes, such as flow under gravity, settling, and film leveling, are stress-driven rather than rate-driven.

An instrument where the shear stress and rate of stress change, rather than the rotational speed, are controlled offers advantages. A few such instruments have existed for many years, eg, the Stormer; others have been developed more recently (173–178). A typical instrument consists of a drag cup motor, a frictionless air-bearing torque shaft, sensors for measuring angular deflection and velocity, and a rotating bob and fixed cup or parallel plates (174–177). The rotating shaft must be suspended in a frictionless manner to permit measurements at very low stresses.

Controlled stress viscometers are useful for determining the presence and the value of a yield stress. The structure can be established from creep measurements, and the elasticity from the amount of recovery after creep. The viscosity can be determined at very low shear rates, often in a Newtonian region. This zero-shear viscosity, η_0, is related directly to the molecular weight of polymer melts and concentrated polymer solutions.

Yield stresses are determined with the help of a vaned cylinder acting as sensor (179), which is attached to a stress rheometer (180). The sensor has four to eight thin blades centered around the cylindrical shaft. The instrument is immersed in the material, and a stress is applied. If the stress is below the yield stress, the material deforms elastically (small strain), but does not yield. When the applied stress exceeds the yield stress, the material flows and the sensor rotates continuously. Usually, a series of measurements are carried out at

successively higher stresses. The yield behavior is seen as a large strain over a short period of time. The torque for yielding is between the last nonyield torque value and the one that produced continuous rotation. Subsequent tests are performed with smaller torque increments to narrow the range for the yield stress. Details of the method and the equation relating yield stress to torque are available (180). Controlled stress techniques are used to determine yield stresses and other flow properties for polymer melts (54) as well as for solutions and dispersions.

Some rotational viscometers employ a disk as the inner member or bob, eg, the Brookfield and Mooney viscometers; others use paddles (a geometry of the Stormer). These nonstandard geometries are difficult to analyze, particularly for an infinite bath, as is usually employed with the Brookfield and the Stormer. The Brookfield disk has been analyzed for Newtonian and non-Newtonian fluids and shear rate corrections have been developed (21). Other nonstandard geometries are best handled by determining instrument constants by calibration with standard fluids.

Pictures and more detailed descriptions are available on the manufacturers' relevant Web sites. Great changes have been made in commercial instruments, particularly in their integration with computers, but a recent paper may point to even greater changes in the future (181). Rheometers generally require actuators to stress specimens and sensors to record the response. However, sensors contribute considerably to the cost and complexity of instruments. A possible alternative to sensors is self-sensing, a technique that involves using knowledge of the actuator's behavior to estimate force or position. Torque or force is self-sensed in some commercial rheometers, but they still need position sensors to measure motion. Since it is possible to self-sense motion of electromagnetic actuators, it should be possible to construct a rheometer having no sensors. Such a rheometer could be small, simple, and inexpensive. To prove their point the authors built a rheometer that fit that description.

4.3. Moving Body Viscometers. In moving body viscometers, the motion of a ball, bubble, plate, needle, or rod through a material is monitored.

Falling ball viscometers are based on Stokes' law, which relates the viscosity of a Newtonian fluid to the velocity of the falling sphere. If a sphere is allowed to fall freely through a fluid, it accelerates until the viscous force is exactly the same as the gravitational force. The Stokes' equation relating viscosity to the fall of a solid body through a liquid may be written as equation 34, where r is the radius of the sphere; d_s and d_l are the density of the sphere and the liquid, respectively; g is the gravitational force; and v is the velocity of the sphere.

$$\eta = \frac{2r^2 g(d_s - d_1)}{9v} \tag{34}$$

Viscometers of the falling ball type can be used over an extremely wide viscosity range, but are usually employed for fairly viscous materials because small balls and small differences in density are needed to obtain a suitably slow rate of fall in a low viscosity fluid. The devices are limited to measurements of Newtonian fluids because no practical formula has been developed for non-Newtonian

materials. They had been considered as instruments for routine viscosity measurements rather than highly accurate work, but more recent designs (182–184) have changed this. The technique has proved to be useful in the study of suspensions, including those that are opaque and concentrated. The cylinder is jacketed for temperature control to within 0.1°C. Optical techniques are used for clear solutions and X-rays for opaque suspensions. A high speed video system is used for recording data.

The speed at which a sphere rolls down a cylindrical tube filled with a fluid or down an angled plate covered with a film of the fluid also gives a measure of viscosity. For the cylindrical tube geometry, equation 35 a generalized form of the Stokes' equation, is used for any given instrument, where v is the translational velocity of the rolling sphere and k is the instrument constant determined by calibration with standard fluids.

$$\eta = \frac{k(d_s - d_l)}{v} \tag{35}$$

The technique of determining viscosity from the velocity of a rolling ball on an inclined plate or panel has been used largely for following the flow, drying, and curing of paints and other coatings (185–187), but can also be used for other materials. The system can be calibrated with standard oils or other fluids of known viscosity. The geometry is ill-defined because the ball often slides and rolls, but the technique is useful. Rolling ball methods based on an inclined plane or an inclined path leading to a horizontal test specimen have been employed to determine the tack of pressure-sensitive adhesives (ASTM D3121) (188–190). The reciprocal of the distance rolled by the ball is considered to be proportional to the tackiness of the adhesive.

Under a broad definition of a moving body, certain other viscometers can be considered to be of this type, including the band, falling rod, falling needle, sliding plate, and bubble tube viscometers. The band viscometer includes an arrangement of parallel plates, the basic geometry used to define shear viscosity. The band, which is a strip of Mylar film, is sandwiched between two fixed plates. The fluid is placed between the band and the plates, and the band is pulled through the fluid. For a given gap and force on the band, the speed of the band is a measure of viscosity.

The falling rod viscometer, though similar to the band viscometer, is based on the movement of a rod rather than a plate through the fluid (191–194). It is a form of a falling coaxial cylinder viscometer. Initially, this device was used for semiempirical studies of materials such as bitumens and rosins. In the 1990s, the Laray falling rod viscometer became a standard test instrument in the ink industry (ASTM D4040), and more recent versions of the falling rod viscometer are capable of precise measurements of polymer melts and solutions (195). In the falling needle viscometer (196,197) (ASTM D5478), the moving body is a glass or stainless steel needle that falls vertically through the fluid. The viscous properties and density of the fluid are derived from the velocity of the needle.

The sliding plate rheometer has been in use for some time, but new types were developed in the 1990s (198–202). The well-defined simple shear

deformation generated by this technique is useful for the characterization of polymer melts and concentrated solutions. Of particular interest is the fact that it can cause a high degree of molecular stretching. The sliding plate rheometer is useful for the characterization of polymer slip at solid boundaries and the determination of the effectiveness of processing aids (203,204).

Viscosity can also be determined from the rising rate of an air bubble through a liquid. This simple technique is widely used for routine viscosity measurements of Newtonian polymer solutions. A bubble tube vicometer consists of a glass tube of a certain size to which liquid is added until a small air space remains at the top. The tube is then capped. When it is inverted, the air bubble rises through the liquid. The rise time may be taken as a measure of viscosity or matched to that of a member of a series of standards (ASTM D1545).

4.4. Other Viscometers. A number of other viscometers are built for specific research or product applications. In one type of design, vibrational techniques are used to measure viscosity. The A&D Weighing SV-10, the Automation Products Dynatrol, and the Nametre are all based on this principle. The SV-10 and the Nametre measure viscosity by monitoring the power required to maintain torsional vibrations in their sensors, two small, thin circular plates for the SV-10 and a small stainless steel rod with a bulb at the end for the Nametre. The Dynatrol determines viscosity by measuring the amplitude of vibration of an immersed flexural member. Because the rate of shear is not easily determined or changed, these instruments are best used for controlling or studying processes in which viscosity changes with time or temperature. In such cases they can be useful because wide ranges of viscosity can be measured without changing sensors (for example, 10^{-1}–10^{6} mPa·s for the Nametre). Special versions of the Dynatrol and Nametre devices are employed for in-line process control for many polymeric solution-based products because of their insensitivity to stirring and flow, wide viscosity ranges, simplicity of design, and ability to be controlled from and transmit data to a remote point.

The Vilastic VE system is based on controlled oscillatory flow in a cylindrical tube. Measurements are performed using oscillatory flow generated at a selected frequency in a precision measurement tube. Viscosity, elasticity, and storage and loss moduli are calculated from data obtained from sensors that monitor the pressure drop across the tube and volume through the tube.

5. Measurement Techniques

5.1. Extensional Viscosity. All three types of extensional viscosity can be measured (107): uniaxial, biaxial, and pure shear. Only a few commercial instruments are available, however, and most measurements are made with improvised equipment. Extensional viscosity of polymer melts can be estimated from converging flow (entrance pressure) or from a melt strength drawdown test (205) as well as measured with techniques described below.

Most uniaxial measurement techniques involve extending a strand or cylindrical rod of the material and measuring the force required. To measure fluids, the fluid is extruded from a spinnerette nozzle and allowed to fall under gravity. It is then extended by being rolled up on a rotating drum (107,206–208).

The generated force is measured by the deflection of the nozzle or tube as the latter is pulled by the filament of fluid or at the take-up roller. This method has been the basis for home-built viscometers and a commercial instrument (208).

Another type of experiment involves a fluid filament being drawn upward against gravity from a reservoir of the fluid (107,209,210), a phenomenon often called the tubeless siphon. The maximum height of the siphon is a measure of the spinnability and extensional viscosity of the fluid. More quantitative measures of stress, strain, and strain rate can be determined from the pressure difference and filament diameter. A more recent technique involves monitoring the stretching of a fluid filament as it is extended (211–216). The basic design is called a filament stretching rheometer (FSR). With a commercial version, the CaBER (Capillary Breakup Extensional Rheometer (Thermo Electron Corp.), a specimen is placed between two parallel plates, and then the upper plate is raised to form a filament. A laser micrometer measures the midpoint diameter of the filament as it thins. The filament breakup time, deformation rate, and extensional viscosity can be calculated from the decrease in diameter with time. All of these methods are limited to spinnable fluids under small total strains and strain rates. High strain rates tend to break the column or filament.

There is another technique that can be used with low viscosity (100 mPa·s) nonspinnable fluids and which allows high strain rates ($> 10^3\ s^{-1}$). A modified opposing jets device (217) is employed that consists of opposing nozzles through which the fluid is sucked or blown out. Extensional viscosity is determined from the force required to keep the nozzles at a fixed distance apart as a function of flow rate. A wide range of fluids can be investigated, and the high strain rates obtainable make it possible to study industrial processes and the effects of low concentrations of additives. A commercial instrument based on this device was on the market for a few years and has been used for some interesting research (218–222).

A sliding plate rheometer (simple shear) can be used to study the response of polymeric liquids to extension-like deformations involving larger strains and strain rates than can be employed in most uniaxial extensional measurements (63,198,202). The technique requires knowledge of both shear stress and the first normal stress difference, $N_1(\dot{\gamma})$, but has considerable potential for characterizing extensional behavior under conditions closely related to those in industrial processes.

Flow entering an orifice from a larger tube produces both shear and extensional deformation of the fluid (223). Although both shear and extensional effects are present, the pressure across the orifice is often dominated by extensional effects. This has been used as the basis for an extensional viscosity attachment for the Vilastic VE tube viscometer (224).

A method for measuring the uniaxial extensional viscosity of polymer solids and melts uses a tensile tester in a liquid oil bath to remove effects of gravity and provide temperature control; cylindrical rods are used as specimens (225,226). The rod extruder may be part of the apparatus and may be combined with a device for clamping the extruded material (227). However, most of the more recent versions use prepared rods, which are placed in the apparatus and heated to soften or melt the polymer (113,228,230). A constant stress or a constant strain

rate is applied, and the resultant extensional strain rate or stress, respectively, is measured. Similar techniques are used to study biaxial extension (107).

In another elongational rheometer (228), the specimen is suspended on the end of a flexible tape, which is wound onto a wheel turned by a servo-controlled torque motor. This design is the basis for the Göttfert Rheostrain instrument. One device for melts and solids is an add-on fixture for rotational rheometers. The SER testing platform (Xpansion Instruments) incorporates dual wind-up drums and can be used for tensile, tear, peel, and friction testing as well as for elongational viscosity measurements.

The Rheometric Melt Elongational Rheometer (RME) is designed for high elongations of polymer melts (231–233). It uses a small (~1 g) compression-molded specimen which it supports on a stream of inert gas and holds in place with a rotary clamping device. The specimen is heated to the test temperature (up to 350°C) by electric heaters and extended by the motion of metal belts. Three sets of belts are available to provide different ranges of extensional strain rates: 10^{-3}–10^{-1} s^{-1}, $3 \times 10^{-3} - 3 \times 10^{-1}$ s^{-1}, and $10^{-2} - 1$ s^{-1}. The force generated by the specimen is measured by a spring-type transducer.

An FSR similar to those becoming popular for measuring the extensional viscosity of fluids has been constructed and applied to polymer melts (234). The FSR results were compared to those obtained from RMEs and agreement was good. Advantages of the FSR include the ability to make measurements on less viscous fluids than with the RME and the use of a smaller size specimen. In addition, the FSR measures all parameters online and very little post-processing of data is necessary. In the RME, a measure of strain during an experiment usually requires observation from a videotape or similar (233).

Biaxial extensional viscosity can be measured by several methods. The most common is bubble inflation, in which a thin polymer sheet is inflated with an inert gas or liquid (235–237). Another method involves stretching a polymer sheet using eight rotating clamps placed in an octagonal pattern (238). A complex servo control system is required to coordinate the motion of the clamps. In a newer technique, displacement is measured as the material is squeezed between two disks having lubricated surfaces (lubricated squeezing flow) (239–244). A commercial instrument based on this technique, the MARS-III Multifunction Axial Rheometer System, has been developed (240). The instrument is computer controlled and data collection is as automatic as the operator wishes.

Extensional viscosity that results purely from shear deformation seems to be of less interest, but has been measured (111). The rheology of several different polymer melts in terms of shear viscosity and uniaxial and biaxial extensional viscosity has been compared (239). Additional information on the measurement of extensional viscosity is also available (108,245,246).

5.2. Viscoelastic Measurement. A number of methods measure the various quantities that describe viscoelastic behavior. Some require expensive commercial rheometers, others depend on custom-made research instruments, and a few require only simple devices. Even qualitative observations can be useful in the case of polymer melts, paints, and resins, where elasticity may indicate an inferior batch or unusable formulation. For example, the extrusion swell of a material from a syringe can be observed with a microscope. The Weissenberg

effect is seen in the separation of a cone and plate during viscosity measurements or the climbing of a resin up the stirrer shaft during polymerization or mixing.

Creep experiments are among the simplest for describing viscoelastic behavior. They involve the measurement of deformation as a function of time after a given load has been applied. Such measurements may be made on specimens in tension, compression, or shear. Many more sophisticated devices exist, including tensile testers. The data are usually presented in the form of a strain–time curve (Figs. 10 and 21). Most materials undergo initial elastic deformation followed by a slow increase in strain with time. After the stress is removed, elastic deformation is recovered, but viscous deformation is not. Creep measurements are useful for evaluating the behavior of structural materials, fasteners, gaskets, pipe, and other articles that are subject to loading while in use. Creep measurements can also be carried out on fluids and are useful for measuring low shear viscosity and elasticity and for estimating and comparing structures, particularly in dispersions such as paints and inks.

Figure 21 is representative of creep and recovery curves for viscoelastic fluids. Such a curve is obtained when a stress is placed on the specimen and the deformation is monitored as a function of time. During the experiment the stress is removed, and the specimen, if it can, is free to recover. The slope of the linear portion of the creep curve gives the shear rate, and the viscosity is the applied stress divided by the slope. A steep slope indicates a low viscosity, and a gradual slope a high viscosity. The recovery part of Figure 21 shows that the specimen was viscoelastic because relaxation took place and some of the strain was recovered. A purely viscous material would not have shown any recovery, as shown in Figure 10**b**.

In a stress–relaxation test the deformation is held constant, and the resulting stress is measured as a function of time. Deformation produces an initial stress that decays with time in the case of viscoelastic materials. In an experiment the sample is rapidly deformed, and the resulting force measured as a function of time. The data may be plotted as stress, stress/initial stress, or modulus (247).

The stress–relaxation process is governed by a number of different molecular motions. To resolve them, the thermally stimulated creep (TSCr) method was developed, which consists of the following steps:

1. The specimen is subjected to a given stress at a temperature T for a time t, both chosen to allow complete orientation of the mobile units that one wishes to consider.
2. The temperature is then lowered to T_0-T, where any molecular motion is completely hindered; then the stress is removed.
3. The specimen is subsequently heated at a controlled rate. The mobile units reorient according to the available relaxation modes. The strain, its time derivative, and the temperature are recorded versus time. By running a series of experiments at different orientation temperatures and plotting the time derivative of the strain rate observed on heating versus the temperature, various relaxational processes are revealed as peaks (248).

In a similar fashion, thermally stimulated current spectrometry (TSC) makes use of an applied d-c potential that acts as the stress to orient dipoles. The temperature is then lowered to trap these dipoles, and small electrical currents are measured during heating as the dipoles relax. The resulting relaxation maps have been related to G' and G'' curves obtained by dynamic mechanical analysis (249–251). This technique, long carried out only in laboratory-built instruments, is available as a commercial TSC spectrometer from Thermold Partners LP, formerly Solomat Instruments (Stamford, Conn.).

Penetration and indentation tests have long been used to characterize viscoelastic materials such as asphalt, rubber, plastics, and coatings. The basic test consists of pressing an indentor of prescribed geometry against the test surface. Most instruments have an indenting tip, eg, cone, needle, or hemisphere, attached to a short rod that is held vertically. The load is controlled at some constant value, and the time of indentation is specified; the size or depth of the indentation is measured. Most instruments make use of a probe geometry which gives an increasing area of contact as penetration proceeds. In this way, at some depth of penetration, the resisting force can become sufficient to balance the applied force on the indentor. Unfortunately, many geometries, eg, diamonds, pyramids, and cones, do not permit the calculation of basic viscoelastic quantities from the results. Penetrometers of this type include the Pfund, Rockwell, Tukon, and Buchholz testers, used to measure indentation hardness which is dependent on modulus.

The Rheo-Tex rheometer is an inexpensive, automated instrument using load cell technology to measure indentation and creep. Available software calculates hardness/softness, brittleness, plasticity, and tensile strength. This instrument is particularly valuable for measurements on foods and personal care products.

Other penetrometer–indentometers include transducers to sense the position and movement of the probe and microprocessors for temperature control and data collection and reduction. These instruments are used mainly to measure softening points, which are not glass transitions but are usually close to those values. Because a softening point is indicative of behavior under load, it is often more useful for predicting performance than the T_g. Penetrometer–indentometers can also be used to measure indentation hardness, creep, creep recovery, and modulus. It has been applied to viscoelastic materials, including polymers and coatings, with excellent results (252–255).

A fully automated microscale indentor known as the Nano Indentor is available from Nano Instruments (256–258). Hardness and elastic modulus are typically measured (258,259) but time-dependent phenomena such as creep and adhesive strength can also be monitored.

Indentation is not usually thought of as a method for measuring viscoelastic properties, but the technique can be useful particularly for measurements of coatings on rigid substrates. A more quantitative technique is called modulus profiling, which uses a modified TMA instrument to measure tensile compliance, a measurement closely related to the inverse of the tensile modulus (260). The instrument can be used to profile or map tensile properties of a polymer specimen to show spatial variations resulting from processing inhomogeneities or aging phenomena such as oxidation.

The most widely used instrument for measuring the viscoelastic properties of solids is the tensile tester or stress–strain instrument, which extends a sample at constant rate and records the stress. Creep and stress–relaxation can also be measured. Numerous commercial instruments of various sizes and capacities are available. They vary greatly in terms of automation, from manually operated to completely computer controlled. Some have temperature chambers, which allow measurements over a range of temperatures. Manufacturers include Applied Test Systems, Benz, Com-Ten Industries, Custom Scientific, Detroit Testing Machine, Dillon Force Measuremet, Dynatek, GRC Instruments, Instron, MTS, Monsanto, SATEC Systems, Inc., Shimadzu, Thwing-Albert, and Tinius Olsen.

A typical stress–strain curve generated by a tensile tester is shown in Figure 22. For more information on tensile testing, consult ASTM methods D2370, D638M, and D882 as well as more recent literature (261,262).

Measurement of the propagation of ultrasonic acoustic waves has been found useful for determining the viscoelastic properties of thin films of adhesives. In this method, the specimen is clamped between transmitting and receiving transducers. The change in pulse shape between successive reverberation of the pulse is dependent on the viscoelastic properties of the transmitting material. Modulus values can be calculated (263,264).

5.3. Dynamic Measurements. Dynamic methods are required for investigating the response of a material to rapid processes, studying fluids, or examining a solid as it passes through a transition region. Such techniques impart cyclic motion to a specimen and measure the resultant response. Dynamic techniques are used to determine storage and loss moduli, G' and G'', respectively, and the loss tangent, tan δ. In addition, the dependence of these moduli can provide insight into polymer architecture (265,266). Some instruments are sensitive enough for the study of liquids and can be used to measure the dynamic viscosity η'. Measurements are made as a function of temperature, time, or frequency, and results can be used to determine transitions and chemical reactions as well as the properties noted above. Dynamic mechanical techniques for solids can be grouped into free vibrations and forced vibrations. Dynamic techniques have been described in detail (247,252,254,262,267–274).

Free-vibration instruments subject a specimen to a displacement and allow it to vibrate freely. The oscillations are monitored for frequency and damping characteristics as they disappear. The displacement is repeated again and again as the specimen is heated or cooled. The results are used to calculate storage and loss modulus data. The torsional pendulum and torsional braid analyzer (TBA) are examples of free-vibration instruments.

The torsional pendulum is a simple apparatus for making dynamic tests in the frequency range of 0.1–10 Hz.

A TBA is a torsional pendulum with which a composite specimen instead of a free film is used (267,270).

With both instruments, data can be plotted as a function of time or temperature to give dynamic mechanical spectra. Such spectra are particularly useful for the study of polymers, including the identification of physical transitions and the onset and kinetics of cross-linking (270,275) or embrittlement (276), as well as for measuring various viscoelastic parameters.

Forced-vibration instruments drive specimens at specific frequencies and determine the response, usually over a range of temperatures. Storage and loss moduli or related parameters are determined. Series of modulus–temperature curves can be generated by making measurements at several different frequencies. Because thermal and mechanical transitions are functions of frequency as well as temperature, data from such curves can be used to calculate activation energies of transitions. In addition, frequencies can be chosen to represent or approximate polymer processing effects and use conditions.

Probably the most common modes of operation are the double cantilever and the tensile mode. In double cantilever, the specimen is held at its ends and driven by a vibrating drive shaft which is clamped to the center of the specimen. In tensile mode the specimen is also clamped at both ends but is driven along the axis between the clamps as one of them is part of the vibrating shaft. With most instruments, several frequencies can be monitored at the same time, as shown in the modulus and tan δ plots of Figure 23. A typical modulus range is $10^3 - 10^{11}$ N/m^2 ($10^4 - 10^{12}$ dyn/cm^2).

5.4. Fluids. The methods described above were designed for solid specimens, although some can be used for fluids if a solid support or carrier is used. The fluid must be highly viscoelastic for data to register, and absolute modulus values are difficult to determine because of the presence of the support. Different instrumentation is needed for the determination of meaningful modulus values over wide viscosity and elasticity ranges. Viscoelastic fluids can be characterized with a number of the rotational viscometers described previously. However, instead of constant rotational motion in one direction, a sinusoidal oscillatory motion must be used. Some oscillatory instruments can act as both dynamic viscometers and dynamic mechanical testing devices. They are capable of making measurements on solids, melts, and relatively concentrated solutions and dispersions. Viscoelasticity can also be determined by a controlled stress rheometer. The shape of a creep curve can show that a fluid is viscoelastic, and the amount of recovery after the stress is removed gives a measure of elasticity.

5.5. Time–Temperature Superposition and Master Curves. Because the modulus of a viscoelastic material varies with time and temperature, measurements must be made over wide ranges of these variables for full characterization. This is often impossible, particularly for very long and very short times. Even if it were possible, the amount of experimental work involved would be prohibitive. Therefore, techniques have been developed to determine modulus values and curves at times or temperatures not attainable experimentally. A series of stress–relaxation, indentation, or modulus curves measured at different temperatures can be shifted on a log time axis to give a single modulus time master curve that covers a wide time range. A creep–compliance–time master curve can be constructed in the same fashion, as can a similar curve by using the families of modulus curves at different frequencies, generated by dynamic mechanical instruments with multiplexing capabilities. These curves can be shifted to a single modulus–frequency master curve because time and temperature have equivalent effects on modulus and other viscoelastic quantities (146,268,269,271–274,277).

Master curves can also be constructed for crystalline polymers, but the shift factor is usually not the same as the one calculated from the WLF equation. An

additional vertical shift factor is usually required. This factor is a function of temperature, partly because the modulus changes as the degree of crystallinity changes with temperature. Because crystallinity is dependent on aging and thermal history, vertical factors and crystalline polymer master curves tend to have poor reproducibility.

Master curves can be used to predict creep resistance, embrittlement, and other property changes over time at a given temperature, or the time it takes for the modulus or some other parameter to reach a critical value. For example, a rubber hose may burst or crack if its modulus exceeds a certain level, or an elastomeric mount may fail if creep is excessive. The time it takes to reach the critical value at a given temperature can be deduced from the master curve. Frequency-based master curves can be used to predict impact behavior or the damping ability of materials being considered for sound or vibration deadening. The theory, construction, and use of master curves have been discussed (146,247, 269,272,273,277,278).

There also is interest in applying the principle of superposition to and developing master curves for polymer solutions. A recent paper (279) describes success in doing so. Measurements of shear viscosity, viscoelasticity, and extensional viscosity were carried out on solutions of polyisobutylene in a solvent consisting of a mixture of polybutene oil and dekalin. Eight solutions were tested, ranging in concentration from 0 to 2.5%. The results showed that both time–temperature and time–concentration superposition held for shear flows. By means of time–concentration superposition, a single master curve could be generated from the various flow curves. A single master curve was not possible for extension dominated flows. Instead, three curves were found, one for each of three concentration regimes, 0–0.1%, 0.25–1.5%, and 2.5%.

6. Practical Rheology

A common problem in rheology is that technologists in charge of research and development, quality control, and problem-solving are rarely trained in rheology, and rheologists are rarely trained in the technology of the product or process. The technologist may use flow to describe effects that are not connected with rheology in the way that a trained rheologist would interpret them. For example, a paint technologist may describe a paint as having poor flow, meaning that the surface has imperfections or defects. However, the same sample may flow easily in a rheological sense during application and cure. The solution of the problem may not involve a change in viscosity, and a small amount of a surfactant may improve the surface appearance of the paint film.

A good working rule in the correlation of viscosity measurements with processing conditions is to select and compare viscosities of materials at the shear rate that corresponds to the process in question. However, problems are encountered with high shear processes. For example, a viscometer with a sufficiently high shear rate may not be available. High shear rates can give heating effects, slip, and erroneous viscosity values. These difficulties can be solved by careful extrapolation from lower shear measurements; Casson plots and other viscosity models can be useful.

Often, a simple ordering of good and poor materials can provide insight into the desired range of viscosity required for satisfactory processing. This strategy assumes that the viscosity of the material is the significant controlling parameter in the process, an assumption that should always be tested. Often, other factors have an equal or even greater influence on the system. For example, in the case of thin films and surfaces, the surface tension and physics of wetting can play a role equal to that of viscosity.

Few processes involve a single shear rate or set of mechanical conditions. Typical processes involve low, intermediate, and high shear regions or sections or stages. For example, a paint or coating may be pumped (intermediate shear rate), be sprayed (high shear rate), coalesce, and flow to form a uniform film (intermediate to low shear rate) and sag or run under gravity (low shear rate) during application. Thus a complete rheological evaluation of a material to determine its processing characteristics requires consideration of the viscosity of the material over an extended shear rate range. A given material may process well at low or intermediate shear rates, but fail completely at higher shear rates.

Additional complications can occur if the mode of deformation of the material in the process differs from that of the measurement method. Most fluid rheology measurements are made under shear. If the material is extended, broken into droplets, or drawn into filaments, the extensional viscosity may be a more appropriate quantity for correlation with performance. This is the case in the parting nip of a roller in which filamenting paint can cause roller spatter if the extensional viscosity exceeds certain limits (280). In many cases shear stress is the key factor rather than shear rate, and controlled stress measurements are necessary.

These examples indicate that the correlation of rheological measurements with product and process performance requires study, knowledge, and hard work (3,8,93,147,162,166,167,281). Extensive applications of rheological measurements have been made to food products (19,93,253,282–285), lubricants (286,287), adhesives (188–190,288–290), paints (8,17,21,42–45,112, 154,163,164,168,171,187,280,291–295), printing inks (1,171,191,194,296–298), rubber (281,299,300), polymers and plastics (46,146,198–204,246,263–274,301), sealants (302), foams (303–306), slurry fuels (307) and other slurries (308,309), cosmetics (93,310), concentrated suspensions (311,315), crude oil (316,317), and powders and granular material (318,319). Careful rheological measurements and a thorough knowledge of the literature should enable the investigator to meet most rheological challenges.

BIBLIOGRAPHY

"Rheology" in *ECT* 1st ed., Vol. 11, pp. 730–748, by J. R. Van Wazer, Monsanto Chemical Co.; "Viscometry" in *ECT* 1st ed., Vol. 14, pp. 756–776, by F. H. Stross and P. E. Porter, Shell Development Corp.; "Rheology" in *ECT* 2nd ed., Vol. 17, pp. 423–444, by J. W. Lyons, Monsanto Co.; "Viscometry" in *ECT* 2nd ed., Vol. 21, pp. 460–484, by R. S. Stearns, Sun Oil Co.; "Rheological Measurements" in *ECT* 3rd ed., Vol. 20, pp. 259–319, by P. E. Pierce and C. K. Schoff, PPG Industries, Inc.; in *ECT* 4th ed., Vol. 21, pp. 347–437, by C. K. Schoff and P. Kamarchik, Jr., PPG Industries, Inc.; "Rheological Measurements" in

ECT (online), posting date: December 4, 2000, by Clifford K. Schoff and Peter Kamarchik, Jr., PPG Industries, Inc.

CITED PUBLICATIONS

1. H. Green, *Industrial Rheology and Rheological Structures*, John Wiley & Sons, Inc., New York, 1949.
2. M. Van Dyke, *An Album of Fluid Motion*, The Parabolic Press, Stanford, Calif., 1982.
3. D. V. Boger and K. Walters, *Rheological Phenomena in Focus*, Elsevier Science Publishing Co., Inc., New York, 1993.
4. H. A. Barnes and K. Walters, *Rheol. Acta* **24**, 323 (1985).
5. C. W. Macosko, in R. J. Goldstein, ed., *Fluid Mechanics Measurements*, Hemisphere Publishing Corp., New York, 1983, p. 423.
6. T. C. Papanastasiou, *J. Rheol.* **31**, 385 (1987).
7. E. A. Collins, C. H. Chen, and J. P. Padolewski, *J. Rheol.* **32**, 163 (1988).
8. R. Eley, in J. Koleske, ed., *Paint Testing Manual: Gardner-Sward Handbook*, 14th ed., ASTM, Philadelphia, 1995, p. 333.
9. J. M. Dealy, *J. Rheol.* **39**, 253 (1995).
10. M. Rosen, *Polym. Plast. Technol. Eng.* **12**(1), 1 (1979).
11. N. Casson, in C. C. Mills, ed., *Rheology of Disperse Systems*, Pergamon Press, New York, 1959, p. 84.
12. W. K. Asbeck, *Off. Dig. Fed. Soc. Paint Technol.* **33**(432), 65 (1961).
13. R. V. Williamson, *Ind. Eng. Chem.* **21**(11), (1929).
14. M. M. Cross, *J. Colloid Sci.* **20**, 417 (1965).
15. Ref. 8, p. 341.
16. W. H. Bauer and E. A. Collins, in F. R. Eirich, ed., *Rheology*, Vol. 4, Academic Press, Inc., New York, 1967, p. 423.
17. O. C. C. Lin, *J. Appl. Polym. Sci.* **19**, 199 (1975).
18. R. Roscoe, in J. J. Hermans, ed., *Flow Properties of Disperse Systems*, North-Holland Publishing Co., Amsterdam, the Netherlands, 1953, p. 1.
19. G. W. Scott Blair, *Elementary Rheology*, Academic Press, Inc., New York, 1969.
20. J. R. Van Wazer, J. W. Lyons, K. Y. Kim, and R. E. Colwell, *Viscosity and Flow Measurement, A Laboratory Handbook of Rheology*, Wiley-Interscience, New York, 1963.
21. P. E. Pierce, *J. Paint Technol.* **43**(557), 35 (1971).
22. M. L. Williams, R. F. Landel, and J. D. Ferry, *J. Am. Chem. Soc.* **77**, 3701 (1955).
23. Z. W. Wicks Jr., G. F. Jacobs, I.-C. Lin, E. H. Urruti, and L. G. Fitzgerald, *J. Coat. Technol.* **57**(725), 51 (1985).
24. Z. W. Wicks Jr., F. N. Jones, and S. P. Pappas, *Organic Coatings: Science and Technology*, Vol. II, John Wiley & Sons, Inc., New York, 1994, p. 13.
25. C. K. Schoff, in J. Brandrup, E. H. Immergut and E. A. Grulke, eds., *Polymer Handbook*, 4th ed., Wiley-Interscience, New York, 1999, p. VII/265.
26. M. L. Huggins, *J. Am. Chem. Soc.* **64**, 2716 (1942).
27. G. V. Schulz and F. Blaschke, *J. Prakt. Chem.* **158**, 130 (1941); *J. Prakt. Chem.* **159**, 146 (1941).
28. P. M. Reilly, B. M. E. van der Hoff, and M. Ziogas, *J. Appl. Polym. Sci.* **24**, 2087 (1979).
29. M. M. Rafi'ee Fanood and M. H. George, *Polymer* **28**, 2244 (1987).
30. K. K. Chee, *J. Appl. Polym. Sci.* **34**, 891 (1987).
31. M. Kurata and Y. Tsunashima, in J. Brandrup, E. H. Immergut, and E. A. Grulke, eds., *Polymer Handbook*, 4th ed., Wiley-Interscience, New York, 1999, p. VII/1.

32. S. H. Aharoni, *J. Appl. Polym. Sci.* **21**, 1323 (1977).
33. J. F. Rabek, *Experimental Methods in Polymer Chemistry*, Wiley-Interscience, New York, 1980.
34. M. Bohdanecky and J. Kovar, *Viscosity of Polymer Solutions*, Elsevier, Amsterdam, the Netherlands, 1982.
35. V. N. Kalashnikov, *J. Rheol.* **38**, 1385 (1994).
36. G. V. Vinogradov and A. Ya. Malkin, *Rheology of Polymers*, Springer-Verlag, New York, 1980.
37. T. G. Fox, S. Gratch, and S. Loshaek, in F. R. Eirich, ed., *Rheology*, Vol. 1, Academic Press, Inc., New York, 1956, p. 431.
38. G. Berry and T. G. Fox, *Adv. Polym. Sci.* **5**, 261 (1968).
39. H. Fujita and Y. Einaga, *Rheol. Acta* **25**, 487 (1986).
40. W. Thimm, C. Friedrich, M. Marth, and J. Honerkamp, *J. Rheol.* **43**, 1663 (1999).
41. W. W. Graessley, in J. E. Mark, ed., *Physical Properties of Polymers*, American Chemical Society, Washington, D.C., 1984, Chapt. 3, p. 97.
42. C. K. Schoff, *Prog. Org. Coat.* **4**, 189 (1976); *Am. Chem. Soc. Div. Polym. Mater. Sci. Eng. Prepr.* **55**, 8 (1986).
43. C. K. Schoff, in Proceedings of the 14th Waterborne and Higher-Solids Coatings Symposium, New Orleans, La., Feb. 1987, p. 252.
44. M. A. Sherwin, J. V. Koleski, and R. A. Taller, *J. Coatings Technol.* **53**(683), 35 (1981).
45. R. Buter, in G. D. Parfitt and A. V. Patsis, eds., in *Proceedings of the Fifth International Conference on Organic Coatings Science and Technology*, Athens, Greece, 1979, Technomics Publishing Co., Westport, Conn., 1981, p. 12.
46. F. N. Cogswell, *Polymer Melt Rheology*, Halsted Press, a division of John Wiley & Sons, Inc., New York, 1981, p. 40.
47. J. M. Dealy and T. O. Broadhead, *Polym. Eng. Sci.* **33**, 1513 (1993).
48. J. L. White, in K. Walters, ed., *Rheometry: Industrial Applications*, Research Studies Press, a division of John Wiley & Sons, Inc., New York, 1980, pp. 209–280.
49. J. M. Dealy and K. F. Wissbrun, *Melt Rheology and Its Role in Plastics Processing*, Van Nostrand Reinhold Co., Inc., New York, 1990.
50. J. Meissner, *Makromol. Chem. Macromol. Symp.* **56**, 25 (1992).
51. J. M. Dealy, *Rheometers for Molten Plastics*, Society of Plastics Engineers and Van Nostrand Reinhold Co., Inc., New York, 1982.
52. B. Maxwell and M. Nguyen, *Polym. Eng. Sci.* **19**, 1140 (1979).
53. B. Maxwell, in C. D. Craver, ed., *Polymer Characterization*, American Chemical Society, Washington, D.C., 1983, p. 149.
54. P. J. Hansen and M. C. Williams, *Polym. Eng. Sci.* **27**, 586 (1987).
55. H. T. Pham and E. Meinecke, *J. Appl. Polym. Sci.* **53**, 257, 265 (1994).
56. N. J. Inkson, T. C. B. McLeish, O. G. Harlen, and D. J. Groves, *J. Rheol.* **43**, 873 (1999).
57. Suneel, R. S. Graham, and T. C. B. McLeish, *Appl. Rheol.* **13**, 19 (2003).
58. T. C. B. McLeish and R. G. Larson, *J. Rheol.* **42**, 81 (1998).
59. W. M. H. Verbeeten, G. W. M. Peters, and H. W. Spiess, *J. Rheol.* **45**, 823 (2001).
60. J. M. Maia, O. S. Carneiro, A. V. Machado, and J. A. Covas, *Appl. Rheol.* **12**, 18 (2002).
61. G. Hay and M. E. Mackay, *J. Rheol.* **43**, 1099 (1999).
62. D. von Dusschoten, M. Wilhelm, and H. W. Spiess, *J. Rheol.* **45**, 1319 (2001).
63. J. G. Oakley and A. J. Giacomin, *Polym. Eng. Sci.* **34**, 580 (1994).
64. F. Koran and J. M. Dealy, *J. Rheol.* **43**, 1279 (1999).
65. S. F. Edwards, *Proc. Phys. Soc., London* **92**, 9 (1967); P. Doi and S. Edwards, *J. Chem. Soc., Faraday Trans. 2* **74**, 1789 (1978).

66. J. Maddox, *Nature* **330**, 11 (1987).
67. J. des Cloizeaux, *Macromolecules* **23**, 4678 (1990).
68. W. W. Graessley, *Acc. Chem. Res.* **10**, 332 (1977).
69. S. H. Wasserman and W. W. Graessley, *J. Rheol.* **36**, 543 (1992).
70. W. H. Tuminello, *Polym. Eng. Sci.* **26**, 1339 (1986); A. Ya. Malkin and A. E. Teishev, *Polym. Eng. Sci.* **31**, 1590 (1992).
71. S. H. Wasserman, *J. Rheol.* **39**, 601 (1995).
72. M. I. Aranguren and co-workers, *J. Rheol.* **36**, 1165 (1992).
73. R. A. Mendelson, *Polym. Eng. Sci.* **8**, 235 (1968); *Polym. Eng. Sci.* **16**, 690 (1976).
74. P. D. Driscoll and D. G. Bogue, *J. Appl. Polym. Sci.* **39**, 1755 (1990).
75. S. E. Kadijk and B. H. A. A. Van Den Brule, *Polym. Eng. Sci.* **34**, 1535 (1994).
76. H. L. Frisch and R. Simha, in F. R. Eirich, ed., *Rheology*, Vol. 1, Academic Press, Inc., New York, 1956, p. 525.
77. I. M. Krieger, in R. Buscall, T. Corner, and I. F. Stageman, eds., *Polymer Colloids*, Elsevier Science Publishing Co., Inc., New York, 1986.
78. S. M. Jogun and C. F. Zukoski, *J. Rheol.* **43**, 847 (1999).
79. J.-D. Lee, J.-H. So, and S.-M. Yang, *J. Rheol.* **43**, 1117 (1999).
80. M. K. Lyon, D. W. Mead, R. E. Elliott, and L. G. Leal, *J. Rheol.* **45**, 881 (2001).
81. A. Sierou and J. F. Brady, *J. Rheol.* **46**, 1031 (2002).
82. J. Mewis, in G. Astarita and co-workers, eds., *Rheology*, Vol. 1, Plenum Press, New York, 1980, p. 149.
83. A. B. Metzner, *J. Rheol.* **29**, 739 (1985).
84. C. Ancey and H. Jorrot, *J. Rheol.* **45**, 297 (2001).
85. I. Zhu, N. Sun, K. Papadopoulos, and D. DeKee, *J. Rheol.* **45**, 1105 (2001).
86. W. B. Russel and P. R. Sperry, *Progr. Org. Coatings* **23**, 305 (1994).
87. T. Shikata and D. S. Pearson, *J. Rheol.* **38**, 601 (1994).
88. J. Persello, A. Magnin, J. Chung, J. M. Piau, and B. Cabanc, *J. Rheol.* **38**, 1845 (1994).
89. N. Phan-Thien, *J. Rheol.* **39**, 679 (1995).
90. T. A. Strivens, *Colloid Polym. Sci.* **261**, 74 (1983).
91. E. Windhab, *Rheology* **2**, 102 (1992).
92. T. Tadros, Chem. Ind. (London), 907 (Dec. 7, 1992).
93. P. Sherman, *Industrial Rheology*, Academic Press, Inc., New York, 1970.
94. D. Quemeda, *Rheol. Acta* **16**, 82 (1977).
95. N. L. Ackermann and H. T. Shen, *AIChE J.* **25**, 237 (1979).
96. M. Mooney, *J. Colloid Sci.* **6**, 162 (1951).
97. D. C.-H. Cheng, Chem. Ind. (London), 408 (May 17, 1980).
98. I. M. Krieger and T. J. Dougherty, *Trans. Soc. Rheol.* **3**, 137 (1959).
99. T. A. Witten and M. F. Cates, *Science* **232**, 1607 (1986).
100. L. M. Sander, *Nature* **322**, 789 (1986).
101. A. A. Catherall, J. R. Melrose, and R. C. Ball, *J. Rheol.* **44**, 1 (2000).
102. J. Mewis and G. Biebaut, *J. Rheol.* **45**, 799 (2001).
103. E. P. Vrahoponlu and A. J. McHugh, *J. Non-Newtonian Fluid Mech.* **25**, 157 (1987).
104. G. I. Taylor, *Proc. R. Soc. Lond., Ser. A* **138**, 41 (1932).
105. Ref. 91, p. 137.
106. J. W. Hill and J. A. Cuculo, *J. Macromol. Sci. C: Rev. Macromol. Chem.* **14**, 107 (1976).
107. J. Ferguson and N. E. Hudson, in R. A. Pethrick, ed., *Polymer Yearbook 2*, Harwood Academic Publishers, London, 1985, p. 155.
108. K. Walters, in P. Moldenaers and R. Keunings, eds., *Theor. Appl. Rheol.*, Vol. 1, Elsevier, Amsterdam, the Netherlands, 1992, p. 16.
109. J. Ferguson and N. E. Hudson, *Int. J. Polym. Mater.* **20**(3–4), 181 (1993).

110. M. Takahashi, T. Isaki, T. Takagawa, and T. Masuda, *J. Rheol.* **37**, 827 (1993).
111. C. D. Denson, *Polym. Eng. Sci.* **13**, 125 (1973).
112. D. F. Massouda, *J. Coatings Technol.* **57**(722), 27 (1985).
113. H. M. Laun and H. Munstedt, *Rheol. Acta* **17**, 415 (1978).
114. K. F. Wissbrun, *Chemtracts: Macromol. Chem.* **1**(2), 131 (1990).
115. J. L. White, *Appl. Polym. Symp.* **33**, 31 (1978).
116. L. Marshall, C. F. Zukoski, and J. Goodwin, *J. Chem. Soc., Faraday Trans.* **185**, 2785 (1989).
117. W. Winslow, *J. Appl. Phys.* **20**, 1137 (1949).
118. N. Webb, *Chem. Br.* **26**, 338 (1990).
119. D. L. Hontsock, R. F. Novak, and G. J. Chaundy, *J. Rheol.* **35**, 1305 (1991).
120. H. Conrad, A. F. Sprecher, Y. Choi, and Y. Chen, *J. Rheol.* **35**, 1393 (1991).
121. W. A. Bullough, *Endeavor.* **14**(4), 165 (1991).
122. T. C. Halsey, *Science* **258**, 761 (1992).
123. R. T. Bonnecaze and J.-F. Brady, *J. Rheol.* **36**, 73 (1992).
124. T. C. Jordan, M. T. Shaw, and T. C. B. McLeish, *J. Rheol.* **36**, 441 (1992).
125. H. Block, *CHEMTECH* **22**, 368 (1992).
126. D. R. Gamota, A. S. Wineman, and F. E. Filisko, *J. Rheol.* **37**, 919 (1993).
127. Z. Lon and R. D. Ervin, *J. Rheol.* **37**, 55 (1993).
128. K. M. Blackwood and H. Block, *Trends Polym. Sci.* **1**(4), 98 (1993).
129. T. C. Halsey, *Adv. Mater.* **5**(10), 711 (1993).
130. E. Westkämper and J. Meschke, *Rheology* **3**, 243 (1993).
131. B. Abu-Jdayil and P. O. Brunn, *Rheology* **4**, 187 (1994).
132. H. Conrad, Y. Li, and Y. Chen, *J. Rheol.* **39**, 1041 (1995).
133. P. J. Rankin and D. J. Klingenberg, *J. Rheol.* **42**, 639 (1998).
134. H. Onihara, Y. Hosoi, K. Tajiri, Y. Ishibashi, M. Doi, and A. Inoue, *J. Rheol.* **43**, 125 (1999).
135. S.-H. Chu and S. J. Lee, *J. Rheol.* **44**, 105 (2000).
136. B. D. Chin and O. O. Park, *J. Rheol.* **44**, 397 (2000).
137. B. Liu and M. T. Shaw, *J. Rheol.* **45**, 641 (2001).
138. H. P. Gavin, *J. Rheol.* **45**, 983 (2001).
139. J. Rabinow, *AIEE Trans.* **67**, 1308 (1948).
140. H. Janocha and B. Rech, *Rheology* **3**, 39 (1993); **4**, 198 (1994).
141. G. J. Besseris, I. F. Miller, and D. B. Yeates, *J. Rheol.* **43**, 591 (1999).
142. Y. M. Shkel and D. J. Klingenberg, *J. Rheol.* **45**, 351 (2001).
143. P. Kuzhir, G. Bossis, and V. Bashtovoi, *J. Rheol.* **47**, 1373, 1385 (2003).
144. C. Zener, *Elasticity and Anelasticity of Metals*, University of Chicago Press, Chicago, Ill., 1948.
145. S. P. Timoshenko and J. N. Goodier, *Theory of Elasticity*, 3rd ed., McGraw-Hill Book Co., Inc., New York, 1969.
146. J. R. Fried, *Polymer Science and Technology*, Prentice Hall Inc., Englewood Cliffs, N.J., 1995.
147. J. Ferguson and Z. Kembłowski, *Applied Fluid Rheology*, Elsevier Science Publishing Co., Inc., New York, 1991.
148. Y. P. Khanna and K. R. Slusarz, *Polym. Eng. Sci.* **33**, 122 (1993).
149. J. K. Gillham and C. K. Schoff, *J. Appl. Polym. Sci.* **20**, 1875 (1976).
150. W. P. Cox and E. H. Merz, *J. Polym. Sci.* **28**, 619 (1958).
151. W. Geissle and B. Hochstein, *J. Rheol.* **47**, 897 (2003).
152. J. Starita, in G. Astarita and co-workers, eds., *Rheology*, Vol. 2, Plenum Press, New York, 1980, p. 229. J. Starita, *Rheometrics System Four*, Rheometrics, Inc., Union, N.J., 1980.
153. J. Meissner, *J. Appl. Polym. Sci.* **16**, 2877 (1972), Weissenberg Rheogoniometer data.

154. O. C. C. Lin, *CHEMTECH* **5**(1), 51 (1975).
155. A. S. Lodge, T. S. R. Al-Hadithi, and K. Walters, *Rheol. Acta* **26**, 516 (1987).
156. A. Ait-Kadi, L. Choplin, and P. J. Carreau, *Polym. Eng. Sci.* **29**, 1265 (1989).
157. G. A. Nuñez, G. S. Ribeiro, M. S. Arncy, J. Feng, and D. D. Joseph, *J. Rheol.* **38**, 1251 (1994).
158. D. Hadjistamov, *Rheology* **5**, 29 (1995).
159. Y. T. Hu and A. Lips, *J. Rheol.* **45**, 1453 (2001).
160. E. B. Bagley, *J. Appl. Phys.* **28**, 624 (1957).
161. R. J. Gardner and P. C. Senanayake, *Rev. Sci. Instrum.* **57**, 3129 (1986).
162. T. C. Patton, *Paint Flow and Pigment Dispersion*, 2nd ed., John Wiley & Sons, Inc., New York, 1979.
163. M. Euverard, *The Efflux Type Viscosity Cup*, Scientific Section, National Paint, Varnish and Lacquer Association, Washington, D.C., 1948.
164. M. Euverard, *ASTM Bull.* **162**, 67 (Oct. 1950).
165. P. E. Pierce, *J. Paint Technol.* **41**(533), 383 (1969).
166. K. Walters, ed., *Rheometry: Industrial Applications*, Research Studies Press, a division of John Wiley & Sons, Inc., New York, 1980.
167. R. W. Whorlow, *Rheological Techniques*, Halsted Press, a division of John Wiley & Sons, Inc., New York, 1980.
168. T. A. Strivens, in R. Lambourne, ed., *Paint and Surface Coatings*, Ellis Horwood Ltd., Chichester, U.K., 1987, Chapt. 14, p. 547.
169. P. Toepke, *Rheology* **1**, 102 (1991).
170. M. Breuker, *Rheology* **1**, 179 (1991).
171. W. Gleissle, *Rheology* **4**, 138 (1994).
172. R. E. Smith, *J. Rheol.* **28**, 155 (1984).
173. S. S. Davis, J. J. Deer, and B. J. Warburton, *Phys. Educ.* **2**, 1 (1968); *J. Pharm. Pharmacol.* **20**, 836 (1968).
174. L. Bohlin, *News Bohlin Rheol.* **2**, 6 (1986).
175. A. J. P. Franck, *J. Rheol.* **29**, 833 (1985).
176. A. J. P. Franck, in *Proceedings of the XI International Congress on Rheology*, Brussels, Belgium, Aug. 1992, p. 982.
177. M. Schmidt and A. J. P. Franck, *Rheology* **4**, 23 (1994).
178. T. S. Wilson, *Appl. Rheol. Meas. Newsl.* **3**(1), 3 (Mar. 1994).
179. Q. D. Nguyen and D. V. Boger, *J. Rheol.* **27**, 331 (1983); *J. Rheol.* **29**, 335 (1985); *Rheol. Acta* **26**, 508 (1987).
180. A. S. Yoshimure, R. K. Prud'homme, H. M. Princen, and A. D. Kiss, *J. Rheol.* **31**, 699 (1987).
181. B. Hanson, M. Levesley and J. Fisher, *Appl. Rheol.* **13**, 242 (2003).
182. L. A. Mondy, A. L. Graham, A. Majumdar, and L. E. Bryant Jr., *Int. J. Multiphase Flow* **12**, 497 (1986).
183. A. L. Graham and co-workers, *Appl. Phys. Lett.* **50**, 127 (1987).
184. B. J. Briscoe, P. F. Luckham, and S. R. Ren, *Colloids Surf.* **62**, 153 (1992).
185. A. Quach and C. M. Hansen, *J. Paint Technol.* **46**(592), 40 (1974).
186. W. Goring, N. Dingerdissen, and C. Hartmann, *Farbe Lack* **83**, 270 (1977).
187. C. K. Schoff, in Proceedings of the 5th Annual ESD Adv. Coatings Conference, Dearborn, Mich., Nov. 1995, p. 77.
188. J. Johnston, *Adhes. Age* **26**, 34 (1983).
189. F. Urushizuki, H. Yamaguchi, and H. Mizumachi, *J. Adhes. Soc. Jpn.* **20**, 195 (1984).
190. H. Mizumachi and T. Saito, *J. Adhes.* **20**, 83 (1986).
191. R. Bassemir, *Am. Inkmaker* **39**(4), 24 (1961).
192. J. Mewis, in Ref. 193, p. 324.
193. G. Pangalos and J. M. Dealy, *J. Oil Colour Chem. Assoc.* **68**(3), 59 (1985).

194. G. Pangalos, J. M. Dealy, and M. B. Lyre, *J. Rheol.* **29**, 471 (1985).
195. K. K. Chee, K. Sato, and A. Rudin, *J. Appl. Polym. Sci.* **20**, 1467 (1976).
196. N. A. Park and T. F. Irvine Jr., *Rev. Sci. Instrum.* **59**, 2051 (1988); *Am. Lab.* **21**(12), 8 (Dec. 1989).
197. N. A. Park and T. F. Irvine, in M. K. Sharma, ed., *Surface Phenomena and Additives in Water-Based Coatings and Printing Technology*, Plenum Press, New York, 1991, p. 241.
198. J. M. Dealy and S. S. Soong, *J. Rheol.* **28**, 355 (1984).
199. S. R. Doshi and J. M. Dealy, *J. Rheol.* **31**, 563 (1987).
200. J. M. Dealy and A. J. Giacomin, in A. A. Collyer and D. W. Clegg, eds., *Rheological Measurement*, Elsevier Applied Science, New York, 1988.
201. A. J. Giacomin, T. Samurkas, and J. M. Dealy, *Polym. Eng. Sci.* **29**, 499 (1989).
202. N. R. Demarquette and J. M. Dealy, *J. Rheol.* **36**, 1007 (1992).
203. S. G. Hatzikiriakos and J. M. Dealy, *J. Rheol.* **35**, 497 (1991); *Int. Polym. Process.* **8**, 36 (1993).
204. I. B. Kazatchov, S. G. Hatzikiriakos, and C. W. Stewart, *Polym. Eng. Sci.* **35**, 1864 (1995).
205. H. M. Laun and H. Schuch, *J. Rheol.* **33**, 119 (1989).
206. C. A. Moore and J. R. A. Pearson, *Rheol. Acta* **14**, 436 (1975).
207. K. M. Baid and A. B. Metzner, *Trans. Soc. Rheol.* **21**, 237 (1977).
208. D. M. Jones, K. Walters, and P. R. Williams, *Rheol. Acta* **26**, 20 (1987).
209. F. D. Martischius, *Rheol. Acta* **21**, 288, 311 (1982).
210. K. K. K. Chao and M. C. Williams, *J. Rheol.* **27**, 451 (1983).
211. M. Stelter and co-workers, *J. Rheol.* **44**, 595 (2000).
212. S. Anna and co-workers, *J. Rheol.* **45**, 83 (2001).
213. S. Anna and G. H. McKinley, *J. Rheol.* **45**, 115 (2001).
214. G. H. McKinley and T. Sridhar, *Ann. Rev. Fluid Mech.* **34**, 375 (2002).
215. M. Stelter and co-workers, *J. Rheol.* **46**, 507 (2002).
216. X. Ye, R. G. Larson, C. Pattamaprom, and T. Sridhar, *J. Rheol.* **47**, 445 (2003).
217. G. G. Fuller, C. A. Cathey, B. Hubbard, and B. F. Zembroski, *J. Rheol.* **31**, 235 (1987).
218. M. R. Anklam, G. G. Warr, and R. K. Prud'homme, *J. Rheol.* **38**, 797 (1994); R. K. Prud'homme and G. G. Warr, *Langmuir* **10**, 3419 (1994).
219. M. E. Mackay, A. M. Dajan, H. Wippel, H. Janeschitz-Kriegl, and M. Lipp, *J. Rheol.* **39**, 1 (1995).
220. S. A. McGlashan, V. T. O'Brien, K. Awati, and M. E. Mackay, *Rheol. Acta* **37**, 214 (1998).
221. S. A. McGlashan and M. E. Mackay, *J. Non-Newtonian Fluid Mech.* **85**, 213 (1999).
222. V. T. O'Brien and M. E. Mackay, *J. Rheol.* **46**, 557 (2002).
223. D. D. Valle, P. A. Tanguy and P. J. Carreau, *J. Non-Newtonian Fluid Mech.* **94**, 1 (2000).
224. Extensional Viscosity and Elasticity of Fluids, Technical Note, Vilastic Scientific, Inc., 2001. Available at www.vilastic.com.
225. R. L. Ballman, *Rheol. Acta* **4**, 137 (1965).
226. F. N. Cogswell, *Rheol. Acta* **8**, 187 (1969).
227. J. Meissner, *Rheol. Acta* **8**, 78 (1969).
228. H. Munstedt, *J. Rheol.* **20**, 211 (1976).
229. H. Munstedt, *J. Rheol.* **23**, 421 (1979).
230. A. Franck and J. Meissner, *Rheol. Acta* **23**, 117 (1984).
231. J. Meissner and J. Hostettler, *Rheol. Acta* **33**, 1 (1994).
232. A. D. Gotsis and M. A. Odriozola, *J. Rheol.* **44**, 1205 (2000).

233. J. S. Schulze, T. P. Lodge, C. W. Macosko, and co-workers, *Rheol. Acta* **40**, 457 (2001).
234. A. Bach, H. K. Rasmussen and O. Hassager, *J. Rheol.* **47**, 429 (2003).
235. C. D. Denson and J. R. Gallo, *Polym. Eng. Sci.* **11**, 174 (1971).
236. D. D. Joye, G. W. Poehlein, and C. D. Denson, *Trans. Soc. Rheol.* **16**, 421 (1972).
237. J. M. Maerker and W. R. Schowalter, *Rheol. Acta* **13**, 627 (1974).
238. J. Meissner, T. Raible, and S. E. Stephenson, *J. Rheol.* **25**, 1, 673 (1981).
239. S. A. Kahn, R. K. Prud-homme, and R. G. Larson, *Rheol. Acta* **26**, 144 (1987).
240. T. C. Hsu and I. R. Harrison, *Polym. Eng. Sci.* **31**, 223 (1991).
241. M. Takahashi, T. Isaki, T. Takagawa, and T. Masuda, *J. Rheol.* **37**, 827 (1993).
242. H. C. Kim, A. Pendse, and J. R. Collier, *J. Rheol.* **38**, 831 (1994).
243. K. Wikström, L. Bohlin, and A.-C. Eliasson, *Rheology* **4**, 192 (1994).
244. N. Golshan Ebrahimi, M. Takahashi, O. Araki, and T. Masuda, *Acta Polym.* **46**, 267 (1995); *J. Rheol.* **39**, 1385 (1995).
245. R. K. Gupta and T. Sridhar, in A. A. Collyer and D. W. Clegg, eds., *Rheological Measurement*, Elsevier Applied Science, New York, 1988, p. 211.
246. J. Meissner, *Rheology* **5**, 120 (1995).
247. J. D. Ferry, *Viscoelastic Properties of Polymers*, 2nd ed., John Wiley & Sons, Inc., New York, 1970.
248. J. C. Monpagens, D. G. Chatain, C. Lacabanne, and P. G. Gautier, *J. Polym. Sci., Polym. Phys. Ed.* **15**, 767 (1977).
249. A. Matthiesen and co-workers, *Amer. Lab.* **23**(1), 44 (Jan. 1991).
250. C. M. Neag, J. P. Ibar, J. R. Saffell, and P. Denning, *J. Coatings Technol.* **65**(826), 37 (1993).
251. J. P. Ibar, P. Denning, T. Thomas, A. Bernes, C. de Goys, J. R. Saffell, P. Jones, and C. Lacabanne, *Polymer Characterization: Physical Property, Spectroscopic, and Chromatographic Methods*, American Chemical Society, Washington, D.C., 1990, p. 167.
252. A. Zosel, *Progr. Org. Coat.* **8**, 47 (1980).
253. A. G. Epprecht, *Farbe Lack* **80**, 505 (1974); *Farbe Lack* **82**, 685 (1976).
254. D. J. Skrovanek and C. K. Schoff, *Progr. Org. Coat.* **16**, 135 (1988).
255. C. K. Schoff and P. Kamarchik, in A. T. Riga and C. M. Neag, eds., *Materials Characterization by Thermomechanical Analysis* (ASTM STP 1136), ASTM, Philadelphia, Pa., 1991, p. 138.
256. G. M. Pharr and W. C. Oliver, *Mater. Res. Soc. Bull.* **17**, 28 (1992).
257. W. C. Oliver, *Mater. Res. Soc. Bull.* **11**, 15 (1986).
258. M. F. Doerner and W. D. Nix, *J. Mater. Res.* **1**, 601 (1986).
259. W. C. Oliver and G. M. Pharr, *J. Mater. Res.* **7**, 1564 (1992).
260. K. T. Gillen, R. L. Clough, and C. A. Quintana, *Polym. Degrad. Stab.* **17**, 31 (1987).
261. Z. W. Wicks Jr., F. N. Jones, and S. P. Pappas, *Organic Coatings Science and Technology*, Vol. II, John Wiley & Sons Inc., New York, 1994, chapt. 24, p. 105.
262. L. W. Hill, in J. V. Koleske, ed., *Paint Testing Manual: Gardner-Sward Handbook*, 14th ed., ASTM, Philadelphia, 1995, p. 534.
263. R. E. Challis, R. P. Cocker, A. K. Holmes, and T. Alper, *J. Appl. Polym. Sci.* **44**, 65 (1992).
264. A. W. Chow and J. L. Bellin, *Polym. Eng. Sci.* **32**, 182 (1992).
265. J. R. Dargan, J. S. Williams and D. N. Lewis, *J. Rheol.* **43**, 1141 (1999).
266. F. Prochazka, D. Durand and T. Nicolai, *J. Rheol.* **43**, 1511 (1999).
267. J. B. Enns and J. K. Gillham, *Computer Applications in Applied Polymer Science*, American Chemical Society, Washington, D.C., 1982, chapt. 20.
268. T. Alfrey Jr., *Mechanical Behavior of High Polymers*, Wiley-Interscience, New York, 1984.

269. J. J. Aklonis, W. J. MacKnight, and M. Shen, *Introduction to Polymer Viscoelasticity*, Wiley-Interscience, New York, 1972.
270. J. K. Gillham, *Developments in Polymer Characterization-3*, Applied Science Publishers, London, 1982, Chapt. 5.
271. N. G. McCrum, B. E. Read, and G. Williams, *Anelastic and Dielectric Effects in Polymer Solids*, John Wiley & Sons, Inc., New York, 1967.
272. L. E. Nielson, *Mechanical Properties of Polymers and Composites*, Vols. 1 and 2, Marcel Dekker, Inc., New York, 1974.
273. A. V. Toblosky, *Properties and Structures of Polymers*, John Wiley & Sons, Inc., New York, 1960.
274. I. M. Ward, *Mechanical Properties of Solid Polymers*, John Wiley & Sons, Inc., New York, 1971.
275. J. K. Gillham, *Polym. Eng. Sci.* **26**, 1429 (1986).
276. C. K. Schoff, *J. Coatings Technol.* **49**(633), 62 (1977).
277. J. M. G. Cowie, *Polymers: Chemistry and Physics of Modern Materials*, International Textbook Co., Ltd., Aylesbury, U.K., 1973, p. 236.
278. E. Catsiff and A. V. Tobolsky, *J. Colloid Sci.* **10**, 375 (1955).
279. A. J. Nogueiro and J. M. Maia, *Appl. Rheol.* **13**, 87 (2003).
280. J. E. Glass, *J. Coatings Technol.* **50**(641), 56, 72 (1978); D. A. Soules, R. H. Fernando, and J. E. Glass, *J. Rheol.* **32**, 181, 199 (1988).
281. J. W. White, *Rubber Chem. Technol.* **42**, 257 (1960).
282. C. Gallegos and M. Berjano, *J. Rheol.* **36**, 465 (1992).
283. K. Seethamraju and M. Bhattacharya, *J. Rheol.* **38**, 1029 (1994).
284. D. Jaros and H. Rohm, *Rheology* **4**, 77 (1994).
285. V. Breton, J. Korolczak, J.-H. Doublier, and J. F. Maingonnat, *Rheology* **5**, 24 (1995).
286. S. M. Goh, M. N. Charalambides, and J. G. Williams, *J. Rheol.* **47**, 701 (2003).
287. E. Kuhn, *Rheology* **4**, 129 (1994).
288. S. Vleeshouwers, A. M. Jamieson, and R. Simha, *Polym. Eng. Sci.* **29**, 662 (1989).
289. M. H. Pahl and D. Hesekamp, *Rheology* **3**, 97 (1993).
290. N. R. Manoj, P. P. De, D. K. Tripathy, and S. K. De, *J. Adhesion Sci. Technol.* **7**, 363 (1993).
291. M. Breucker, *Rheology* **3**, 48 (1993).
292. M. Osterhold and Y. Jäger, *Rheology* **3**, 250 (1993).
293. N. Leskovsek, L. Tusar, and M. Tusar, *Rheology* **5**, 140 (1995).
294. J. E. Glass and R. K. Prud'homme, in S. F. Kistler and S. M. Schweitzer, eds., *Liquid Film Coating*, Chapman & Hall, London, 1996, p. 137.
295. M. Osterhold, *Eur. Coat. J.* **2000**, 206 (2000).
296. Y.-H. Zang, J. S. Aspler, M. Y. Boluk, and L. H. DeGrâce, *J. Rheol.* **35**, 345 (1991).
297. T. Hartford, *Am. Inkmaker* **72**(11), 42 (1994).
298. M. Fernández and co-workers, *J. Rheol.* **42**, 239 (1998).
299. M. H. Wagner and J. Schaeffer, *J. Rheol.* **37**, 643 (1993).
300. A. Roychoudhury and S. K. De, *J. Appl. Polym. Sci.* **50**, 811 (1993).
301. G. Sanz, *J. Appl. Polym. Sci.* **55**, 75 (1995).
302. E. A. Collins, C. H. Chen, and J. P. Padolewski, *J. Rheol.* **32**, 163 (1988); *J. Rheol.* **36**, 117, 131 (1992).
303. A. M. Kraynik and M. G. Hansen, *J. Rheol.* **31**, 175 (1987).
304. E. Mora, L. D. Artavia, and C. W. Macosko, *J. Rheol.* **35**, 921 (1991).
305. A. M. Kraynik, D. A. Reinelt, and H. M. Prince, *J. Rheol.* **35**, 1235 (1991).
306. T. Okuzono, K. Kawasaki, and T. Nagai, *J. Rheol.* **37**, 571 (1993).
307. S.-F. Lin and R. S. Brodkey, *J. Rheol.* **29**, 147 (1985).
308. R. J. Mannheimer, *J. Rheol.* **35**, 113 (1991).
309. M. K. Agarwala, B. R. Patterson, and P. E. Clark, *J. Rheol.* **36**, 319 (1992).

310. D. Holland, *Rheology* **2**, 108 (1991).
311. J. Schröder, *Rheology* **2**, 40 (1992).
312. S. A. Khan and N. J. Zoeller, *J. Rheol.* **37**, 1225 (1993).
313. D. M. Kalyon, *CHEMTECH* **25**(5), 22 (May 1995).
314. R. L. Hoffman, *J. Rheol.* **42**, 111 (1998).
315. P. Pignon, A. Magnin and J.-M. Piau, *J. Rheol.* **42**, 1349 (1998).
316. L. T. Wardhaugh and D. V. Boger, *AIChE J.* **37**, 871 (1991).
317. L. E. Sanchez and J. L. Zakin, *Ind. Eng. Chem. Res.* **33**, 3256 (1994).
318. R. Ocone and G. Astarita, *J. Rheol.* **37**, 727 (1993).
319. Y. Tomita, H. Ikeuchi, S. Kuchii, and K. Funatsu, *J. Rheol.* **38**, 231 (1994).

GENERAL REFERENCES

References (8,10,19,20,36,46,47,51,93,146,154,162,166–168,247,268,269,271–274), and 277 are good general references.
Reference 20, although out of date, is the single-most useful reference in this area. References 42 and 51 are good references for viscometers in general.

H. A. Barnes, J. F. Hutton, and K. Walters, *An Introduction to Rheology*, Elsevier Applied Science, New York, 1989.
B. D. Coleman, H. Markovitz, and W. Noll, *Viscometric Flow of Non-Newtonian Fluids*, Springer-Verlag, New York, 1966.
A. A. Collyer, ed., *Techniques in Rheological Measurement*, Chapman and Hall, New York, 1993.
A. A. Collyer and D. W. Clegg, eds., *Rheological Measurement*, Elsevier Applied Science, New York, 1988.
A. Dinsdale and R. Moore, *Viscometry and Its Measurement*, The Institute of Physics and the Physical Society, Reinhold Publishing Corp., New York, 1963.
F. R. Eirich, ed., *Rheology: Theory and Application*, Vols. 1–5, Academic Press, Inc., New York, 1956–1970.
A. G. Fredrickson, *Principles and Applications of Rheology*, Prentice-Hall, Inc., Englewood Cliffs, N.J., 1964.
C. W. Macosko, ed., *Rheology: Principles, Measurements, and Applications*, VCH Publishers, Inc., New York, 1994. An excellent text and reference.
T. G. Mezger, *The Rheology Handbook*, Vincentz Verlag, Hannover, 2002. An excellent resource for users and potential purchasers of rotational and oscillatory rheometers.
M. Reiner, *Deformation, Strain and Flow*, 2nd ed., Interscience Publishers, New York, 1960.
M. Rosen, *Polym. Plast. Technol. Eng.* **12**(1), (1979). A very useful, practical review.
S. Ross and I. D. Morrison, *Colloidal Systems and Interfaces*, John Wiley & Sons, Inc., New York, 1988.
W. R. Schowalter, *Mechanics of Non-Newtonian Fluids*, Pergamon Press, New York, 1977.
K. Walters, *Rheometry*, Halsted Press, a division of John Wiley & Sons, Inc., New York, 1975.

There are a number of excellent journals that cover or include rheological studies. Two particularly useful ones are the *Journal of Rheology* (free with membership in the Society of Rheology, see www.rheology.org/sor/) and *Applied Rheology* (www.ar.ethz.ch), which provides an excellent combination of papers,

new equipment descriptions, announcements, abstracts of dissertations and papers, and other information. Other useful journals include *Rheologica Acta, Polymer Engineering and Science*, and the *Journal of Applied Polymer Science*.

CLIFFORD K.SCHOFF
Schoff Associates
PETER KAMARCHIK JR.
PPG Industries

Table 1. **Flow Equations for Flow Models**

Flow model	Flow equation
Newtonian	$\tau = \eta\dot{\gamma}$
plastic (Bingham) body	$\tau - \tau_0 = \eta\dot{\gamma}$
power law	$\tau = k\lvert\dot{\gamma}\rvert^n$
power law with yield value	$\tau - \tau_0 = k\lvert\dot{\gamma}\rvert^n$
Casson fluid	$\tau^{1/2} - \tau_0^{11/2} = \eta_\infty^{1/2}\dot{\gamma}\rvert^{1/2}$
Williamson	$\eta = \eta_\infty + \dfrac{(\eta_0 - \eta_\infty)}{1 + \frac{[r]}{r_m}}$
Cross	$\eta = \eta_\infty + \dfrac{(\eta_0 - \eta_\infty)}{1 + \alpha\dot{\gamma}^n}$

Table 2. **Viscosity Expressions**

Common name	Recommended name	Definition	Common units
relative viscosity	viscosity ratio	$\eta_{\text{rel}} = t/t_0 = \eta/\eta_0$	none
specific viscosity		$\eta_{\text{sp}} = (\eta - \eta_0)/\eta_0 = \eta^{-1}{}_{\text{rel}}$	none
reduced viscosity	viscosity number	$\eta_{\text{red}} = \eta_{\text{sp}}/c = (\eta^{-1}{}_{\text{rel}})/c$	dL/g
inherent viscosity	logarithmic viscosity number	$\eta_{\text{inh}} = (\ln \eta_{\text{rel}})/c$	dL/g
intrinsic viscosity	limiting viscosity number	$[\eta] = \text{limit}_{c\to 0}\frac{\eta_{\text{rel}}}{c} = \text{limit}_{c\to 0}\frac{\ln \eta_{\text{rel}}}{c}$	dL/g

Table 3. **Measured Values of Elastic Constants at Small Extensions and 25°C**[a]

Material	Young's modulus, E, GPa[b]	Proportionality limit[c] % extension	Shear modulus, G, GPa[b]	Poisson's ratio, μ	Bulk modulus, B, GPa[b]
vitreous silica	70.0	3	30.5	0.14	37.4
mild steel	200–220	2.5	76–83	0.29	160.0
brass	80–100	2	26–38	0.25–0.4	61
Constantan	163	2	61	0.33	160.0
nickel	200–220	2	78–80	0.30	170.0
tin	39–55		17–20	0.33	52
silver	60–80	2	24–28	0.38	100
granite	ca 30	0.5	ca 10	ca 0.3	ca 30
gelatin gel[d]	2×10^{-4}	10		0.50	
dry wood	4–18	1			
axial	~ 1	1			
piece					
radial					
piece					
silk thread	6.4	1			
natural rubber	8.6×10^{-4}	400–600	2.9×10^{-4}	0.49	0.019
hard rubber	0.36	3			
phenolic resin, mineral-filled	2.4	2			
nylon	0.31	3			
polyethylene	0.010	2			

[a] Ref. 20.
[b] To convert GPa to psi, multiply by 145,000.
[c] Values are approximate.
[d] 80% H_2O.

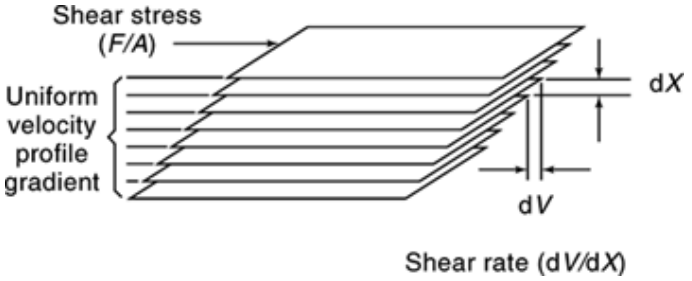

Fig. 1. Laminar flow in simple shear. $F/A = \eta\, dV/dX$, where F is the force acting on area A, V the velocity and X the thickness of the layer, and η the coefficient of viscosity or the Newtonian viscosity.

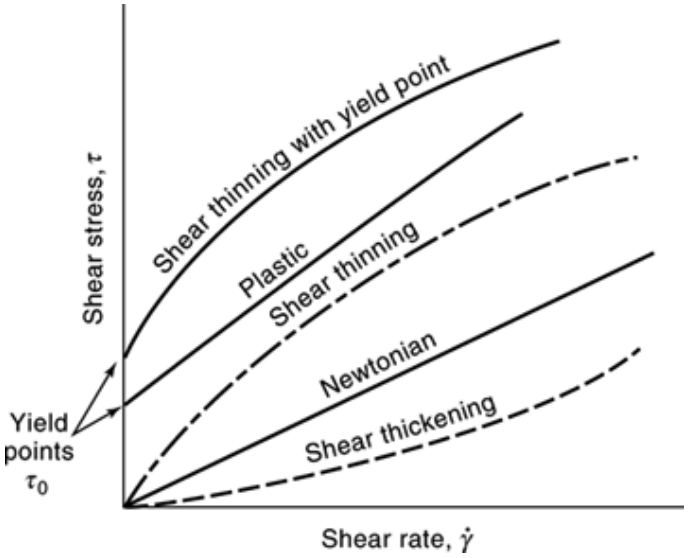

Fig. 2. Flow curves (shear stress vs shear rate) for different types of flow behavior.

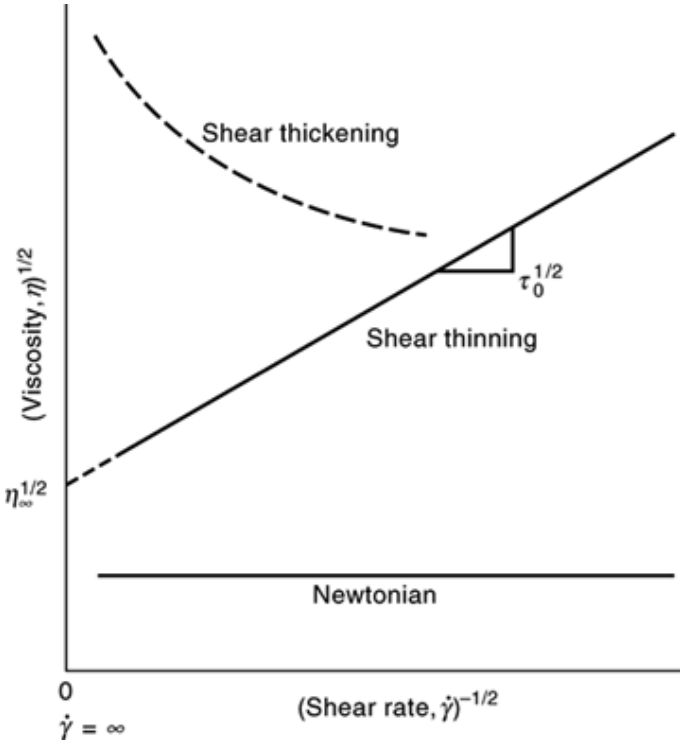

Fig. 3. Examples of Casson plots: (viscosity)$^{1/2}$ vs (shear rate)$^{-1/2}$. The Casson equation is $\eta^{1/2} = \eta_\infty{}^{1/2} + \tau_0{}^{1/2}\gamma^{-1/2}$.

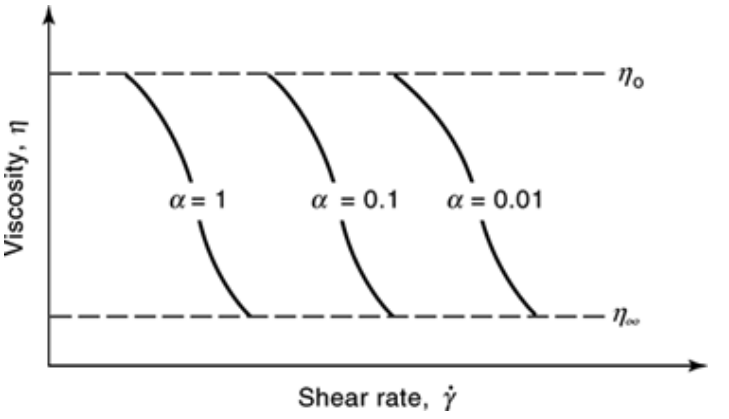

Fig. 4. Graphic representations (viscosity vs shear rate) of Cross model with different values for α.

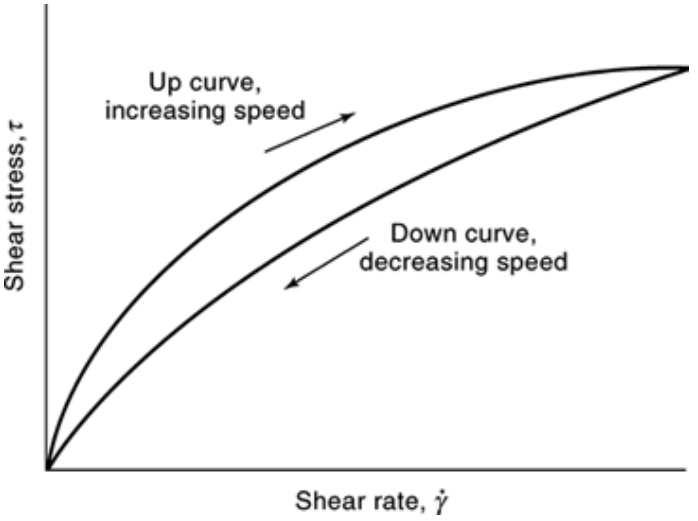

Fig. 5. Flow curves (up and down) for a thixotropic material: hysteresis loop.

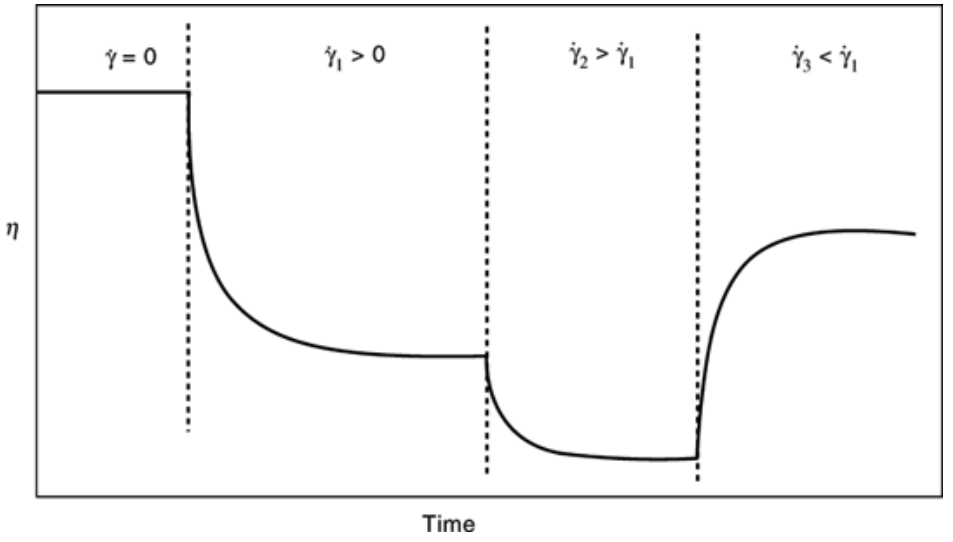

Fig. 6. Viscosity–time effects for a thixotropic material at rest ($\gamma = 0$), at some shear rate, $\gamma\cdot$, at an increased shear rate, and then at a lower shear rate.

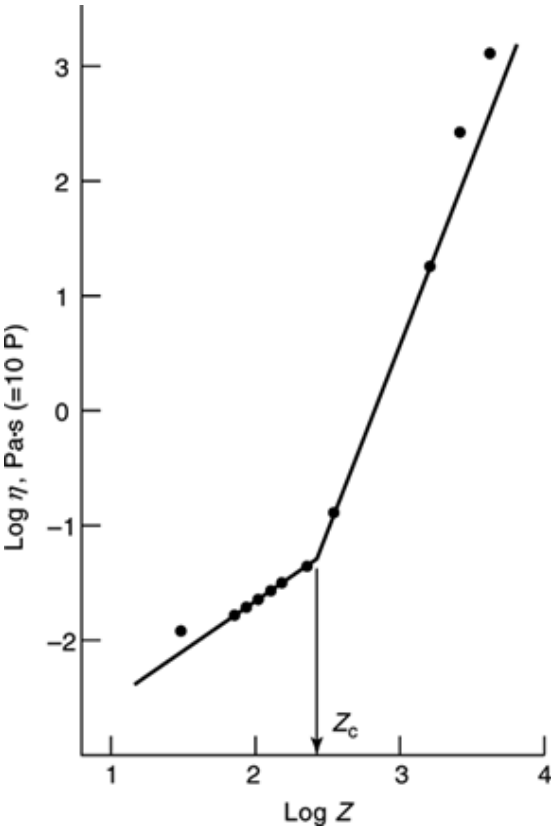

Fig. 7. Newtonian viscosity vs chain length in terms of the number of carbon atoms for a series of molten polyethylenes. To convert Pa·s to P, multiply by 10. Courtesy of Springer Verlag.

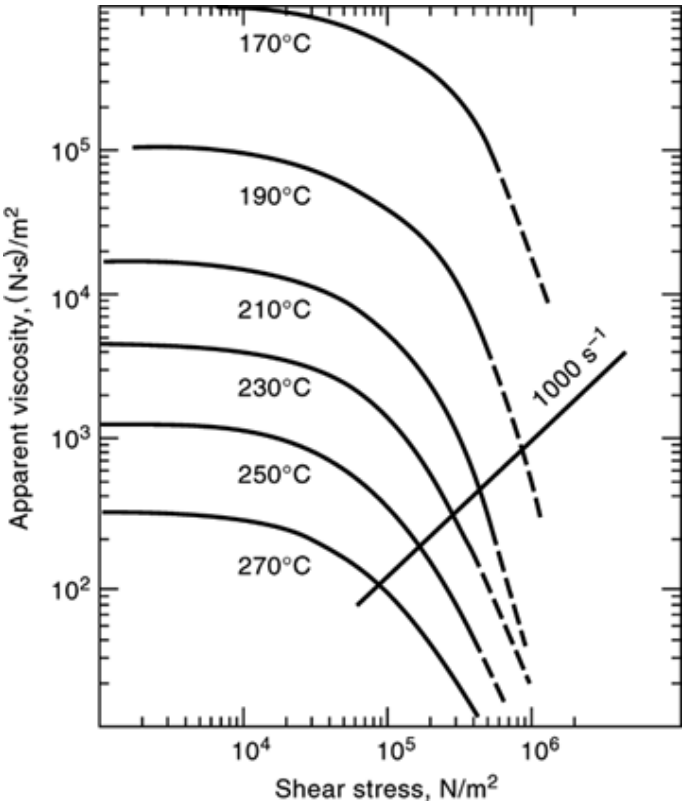

Fig. 8. Viscosity at different temperatures measured by a capillary viscometer: injection-molding grade of poly(methyl methacrylate) (46). To convert N/m^2 to psi, multiply by 145; to convert $(N \cdot s)/m^2$ to $(dyn \cdot s)/cm^2$(P), multiply by 10.

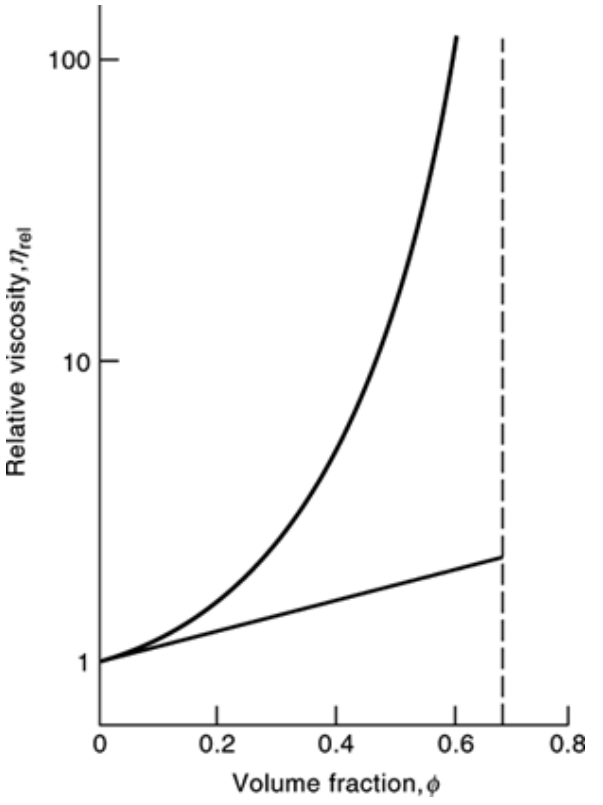

Fig. 9. Relative viscosity vs volume fraction for a typical dispersion (curved line), where the solid straight line represents the Einstein relationship $[\eta] = 2.5$, and the dashed line is an approximate value for the limiting volume fraction ϕ_m.

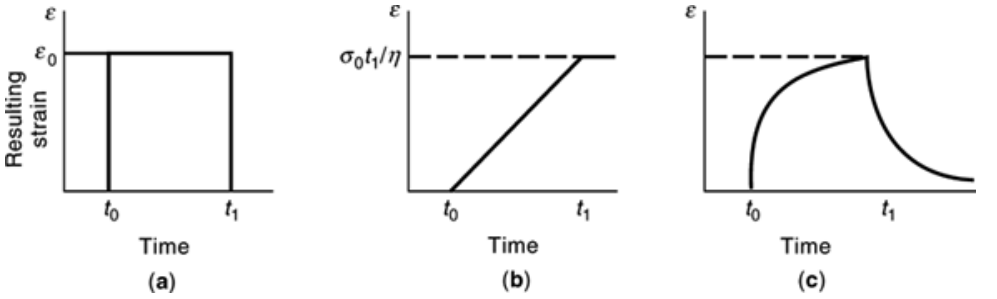

Fig. 10. Response (strain) of different idealized materials to an instantaneous application of a stress at time $t = t_0$: (**a**) elastic, (**b**) viscous, and (**c**) viscoelastic.

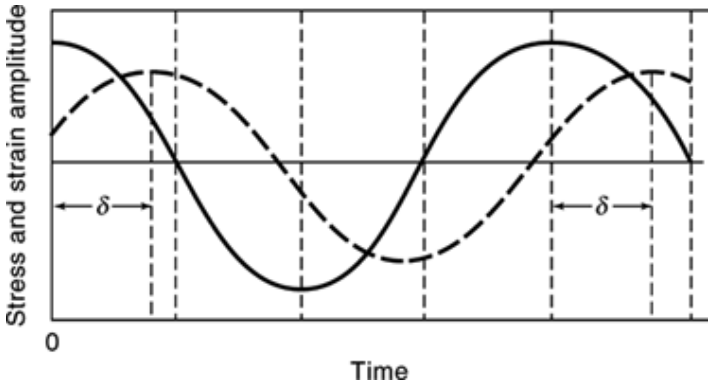

Fig. 11. Viscoelastic material: stress (—) and strain (---) amplitudes vs time where δ is the phase angle that defines the lag of the strain behind the stress.

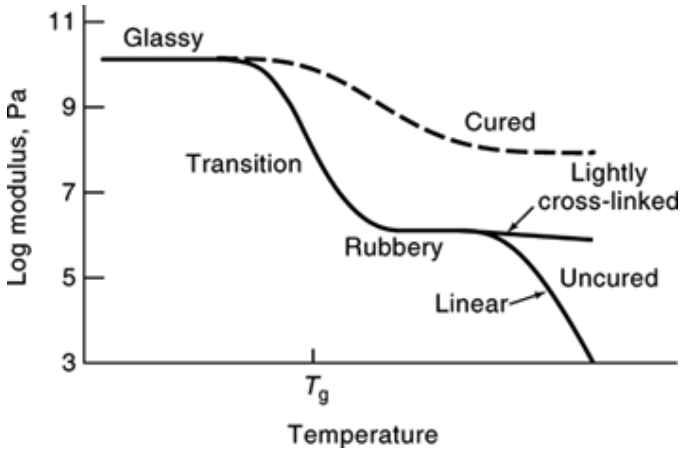

Fig. 12. Generalized modulus–temperature curves for polymeric materials, showing the high modulus glassy state, glass-transition regions for cured and uncured polymers, plateau regions for cross-linked polymers, and the drop-off in modulus for a linear polymer.

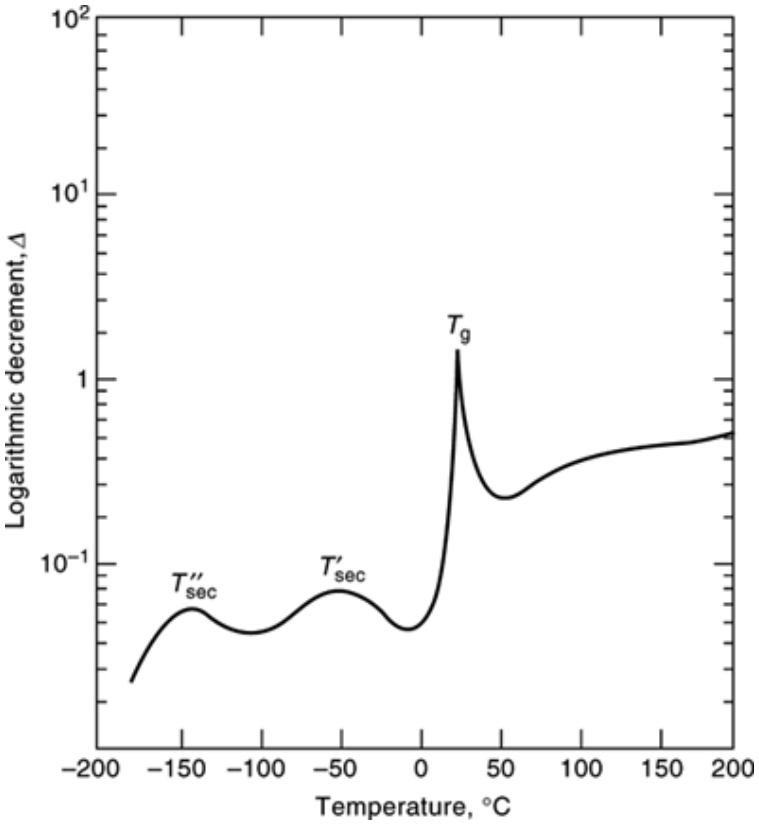

Fig. 13. Logarithmic decrement (related to tan δ and loss modulus) vs temperature for a fluorocarbon dibenzoxazole (149). After drying up to 200°C, the experiment was conducted at 200 → −180 → 200°C:$\Delta T/\Delta t = \pm 1.5$°C/min in a helium atmosphere. The T_g gives a sharp damping peak, whereas the secondary glassy state transitions, T_{sec}, are very broad.

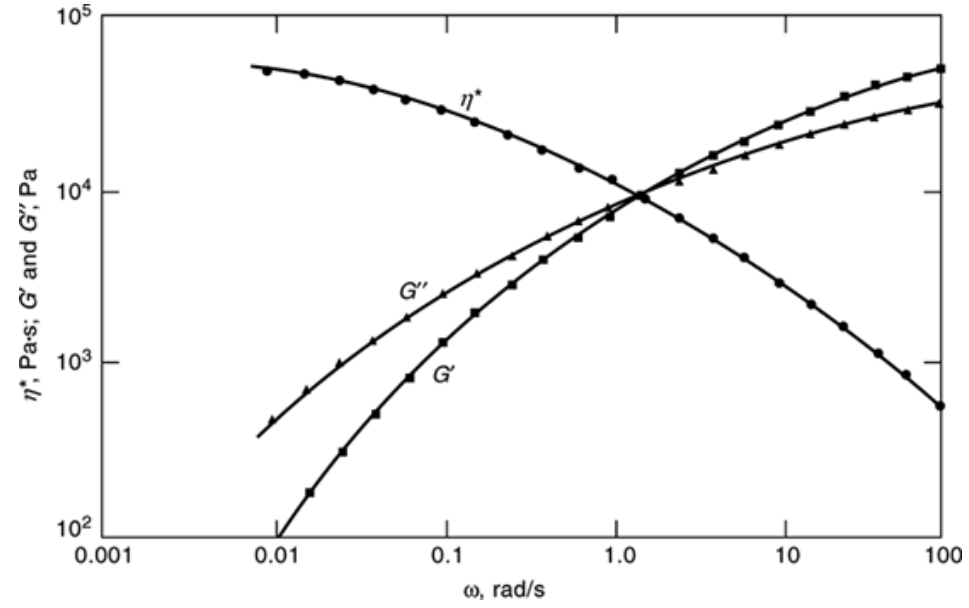

Fig. 14. Dynamic viscoelastic properties of a low density polyethylene (LDPE) at 150°C: complex dynamic viscosity η^*, storage modulus G', and loss modulus G'' vs angular velocity, ω. To convert Pa·s to P, multiply by 10; to convert Pa to dyn/cm^2, multiply by 10. Courtesy of Rheometric Scientific.

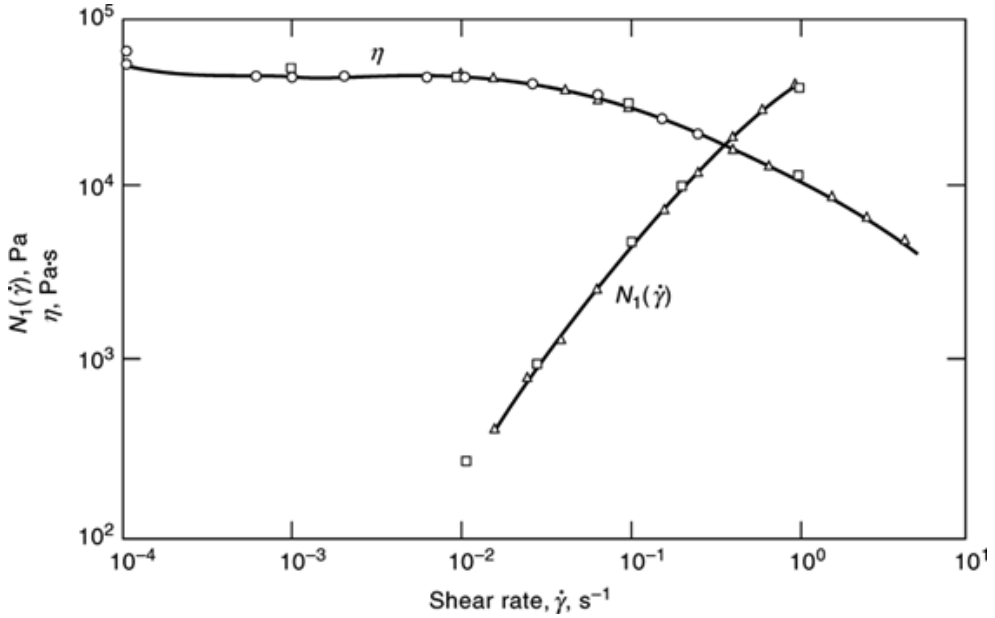

Fig. 15. Shear viscosity η and first normal stress difference $N_1(\gamma\cdot)$ vs shear rate $\gamma\cdot$ for a low density polyethylene at 150°C (152,153), where | parallel plate; Δ cone and plate; and □: Weissenberg rheogoniometer. To convert Pa to dyn/cm^2, multiply by 10; to convert Pa·s to P, multiply by 10. Courtesy of *Rheometric Scientific*.

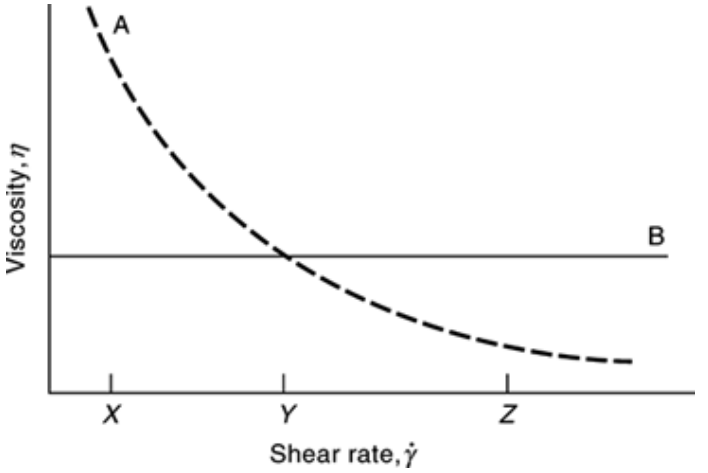

Fig. 16. Viscosity vs shear rate curves for two fluids, showing the fallacy of a single-point measurement. Fluid A would appear to be more viscous than fluid B if measured only at point *X*, of the same viscosity if measured at point *Y*, and less viscous if measured only at point *Z*.

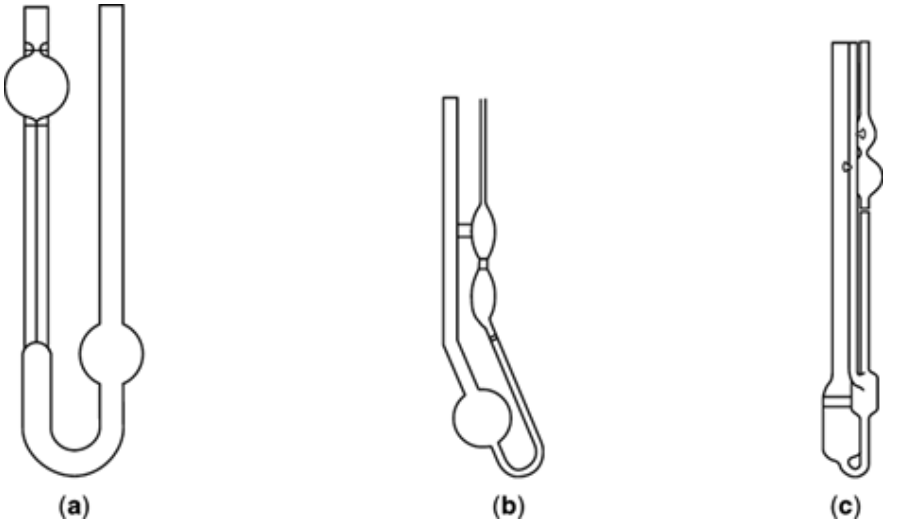

Fig. 17. (**a**) Ostwald glass capillary viscometer, (**b**) Cannon–Fenske viscometer, and (**c**) Ubbelohde viscometer.

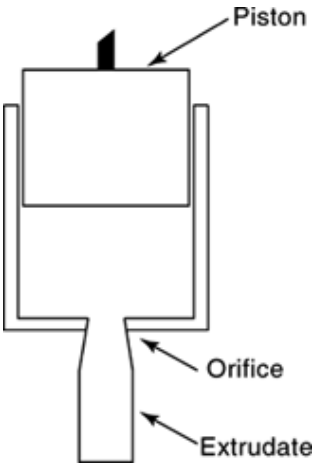

Fig. 18. Piston cylinder capillary viscometer (51).

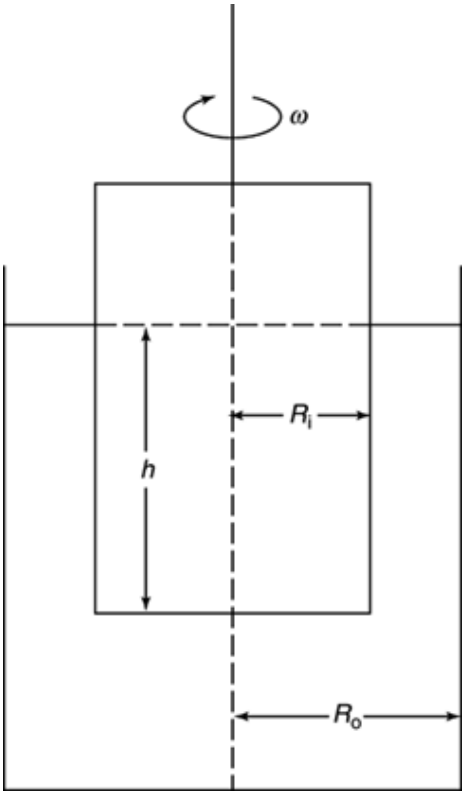

Fig. 19. Concentric cylinder viscometer. R_i and R_o are the radii of the inner and outer cylinder, respectively, and ω is the relative angular velocity.

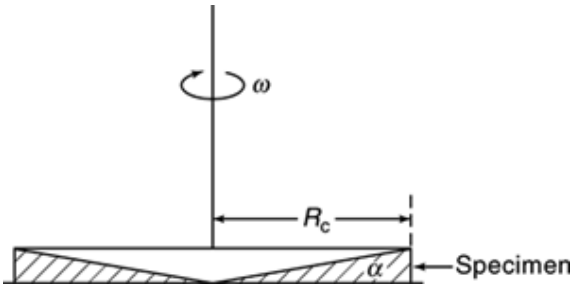

Fig. 20. Cone–plate viscometer. R_c is the radius of the cone, α is the angle between cone and plate, and ω is the relative angular velocity.

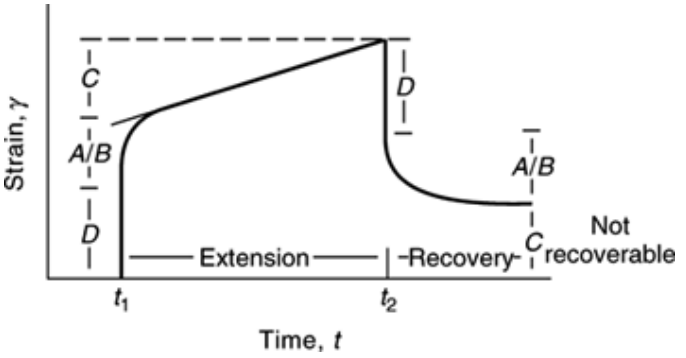

Fig. 21. Typical creep curve for a viscoelastic material. Stress applied at time t_1 and removed at t_2.

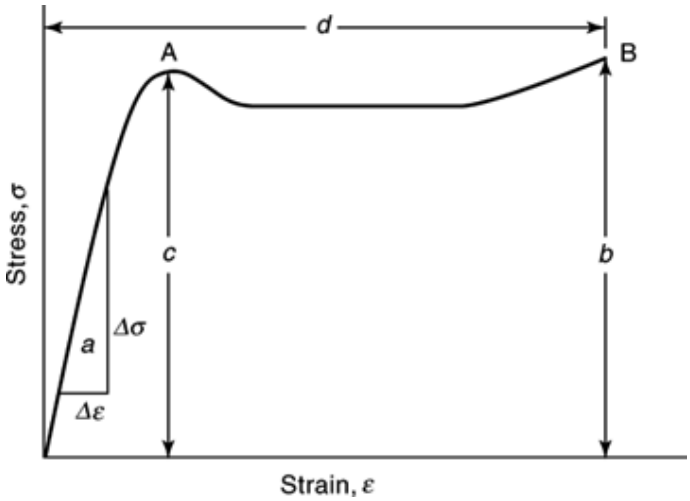

Fig. 22. Typical stress–strain curve. Point A is the yield point of the material; the sample breaks at point B. Mechanical properties are identified as follows: $a = \Delta\sigma/\Delta\partial$, modulus; $b =$ tensile strength; $c =$ yield strength; $d =$ elongation at break. The toughness or work to break is the area under the curve.

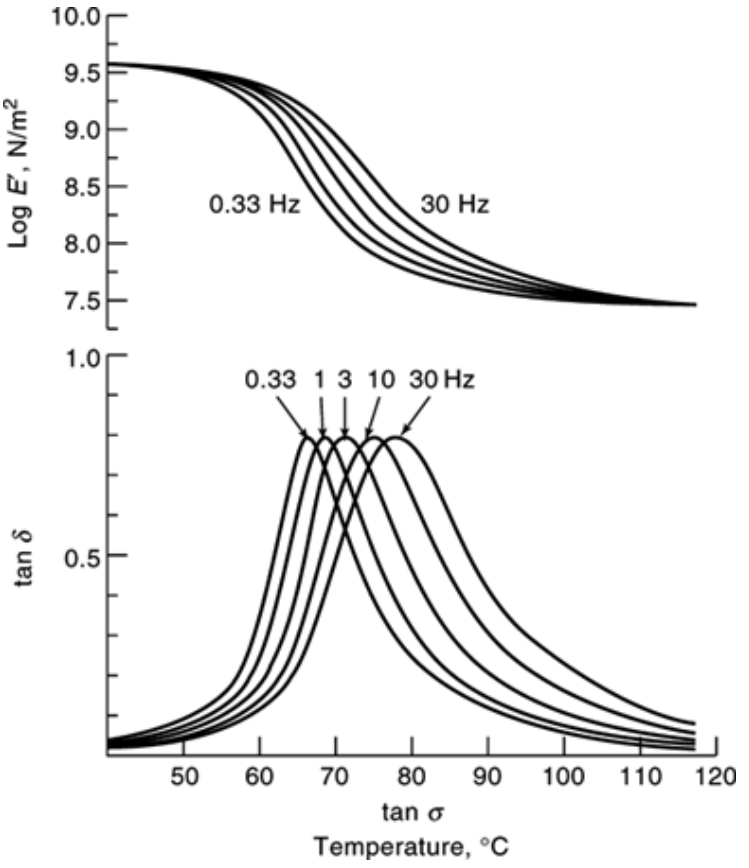

Fig. 23. Multifrequency modulus and tan δ vs temperature plots. To convert N/m^2 to, multiply by 1.45×10^4.